DECOLORIZATION AND COD REDUCTION OF THE EFFLUENT FROM BIOGAS CHAMBER BY ADVANCED ELECTRO-FENTON PROCESS

BY

MS. PREENAPHAN TANTEERAPOLCHAI

A THESIS SUBMITTED IN PARTIAL FULFILLMENT OF THE REQUIREMENTS FOR THE DEGREE OF MASTER OF ENGINEERING (ENGINEERING TECHNOLOGY)

SIRINDHORN INTERNATIONAL INSTITUTE OF TECHNOLOGY

THAMMASAT UNIVERSITY

ACADEMIC YEAR 2020

DECOLORIZATION AND COD REDUCTION OF THE EFFLUENT FROM BIOGAS CHAMBER BY ADVANCED ELECTRO-FENTON PROCESS

BY

MS. PREENAPHAN TANTEERAPOLCHAI

A THESIS SUBMITTED IN PARTIAL FULFILLMENT OF THE REQUIREMENTS FOR THE DEGREE OF MASTER OF ENGINEERING (ENGINEERING TECHNOLOGY)
SIRINDHORN INTERNATIONAL INSTITUTE OF TECHNOLOGY
THAMMASAT UNIVERSITY
ACADEMIC YEAR 2020

THAMMASAT UNIVERSITY
SIRINDHORN INTERNATIONAL INSTITUTE OF TECHNOLOGY

THESIS

BY

MS. PREENAPHAN TANTEERAPOLCHAI

ENTITLED

DECOLORIZATION AND COD REDUCTION
OF THE EFFLUENT FROM BIOGAS CHAMBER
BY ADVANCED ELECTRO-FENTON PROCESS

was approved as partial fulfillment of the requirements for
the degree of Master of Engineering (Engineering Technology)

on June 2, 2021

Chairperson
WINARTO KURNIAWAN
(Assistant Professor Winarto Kurniawan, Ph.D.)

Member and Advisor
(Associate Professor Paiboon Sreearunothai, Ph.D.)

Member and Co-advisor
กรกช สมบัติมั่นคง
(Korakot Sombatmankhong, Ph.D.)

Member
(Associate Professor Pakorn Opaprakasit, Ph.D.)

Director
(Professor Pruettha Nanakorn, D.Eng.)

Thesis Title	DECOLORIZATION AND COD REDUCTION OF THE EFFLUENT FROM BIOGAS CHAMBER BY ADVANCED ELECTRO-FENTON PROCESS
Author	Ms. Preenaphan Tanteerapolchai
Degree	Master of Engineering (Engineering Technology)
Faculty/University	Sirindhorn International Institute of Technology/ Thammasat University
Thesis Advisor	Associate Professor Paiboon Sreearunothai, Ph.D.
Thesis Co-Advisor	Korakot Sombatmankhong, Ph.D.
Academic Year	2020

ABSTRACT

This thesis studies the decolorization and chemical oxygen demand (COD) reduction feasibility of the effluent from the biogas chamber by the advanced electro-Fenton (AEF) process, which generates powerful hydroxyl radicals that can degrade the highly colored compound (melanoidin) and concentration of organic matter in the effluent.

Electro-Fenton process (traditional electro-Fenton (TEF) process) can produce hydroxyl radicals ($^{\bullet}OH$) by the continuous electro-generation of hydrogen peroxide (H_2O_2) on the cathode via oxygen reduction and the addition of ferrous (Fe^{2+}), which can oxidize most refractory organic pollutants in biogas effluent efficiently. The advantage of electro-Fenton process compare to the Fenton process, the electro-Fenton process include producing hydrogen peroxide (H_2O_2) without adding an expensive H_2O_2 reagent into the system and easily monitoring electricity. However, from the thesis results, the traditional electro-Fenton (TEF) process showed low efficiencies of the decolorization and COD reduction. In order to reveal the play role of foam nickel can produce superoxide anion ($\bullet O_2^-$) to react with hydrogen peroxide (H_2O_2) for generating hydroxyl radicals which enhance degradation efficiency. Therefore, the advanced electro-Fenton (AEF) process by adding foam nickel in the traditional electro-

Fenton (TEF) process was introduced to treat the effluent from the biogas chamber to achieve the most effective color and COD removal efficiencies.

The studied parameters were also investigated to find the optimum condition in this thesis by using the advanced-electro-Fenton process which included initial pH (2-11), initial ferrous concentration (0.5-9 mM), applied voltage (1.0-4.0V), and reaction time (0-300 minutes) under ambient temperature.

According to the experimental results, the advanced electro-Fenton (AEF) process proved to be the most effective treatment process for decolorization and COD reduction, compared with advanced electrochemical (AEM) process, traditional electro-Fenton (TEF) process, and advanced electro-Fenton process without applied voltage (AEF_0V). The optimum condition for decolorization and COD reduction by the advanced electro-Fenton process was observed at the initial pH of 3, the initial ferrous concentration of 3 mM, the applied voltage of 2.0V, and 120 minutes of the reaction time. The efficiency of decolorization was found to be 87.6±0.5%, in which the color value was reduced from 14,250±250 to 1,767±58ADMI. The efficiency of COD reduction was 73.7±1.1%, in which COD value was dropped from 5,067±230 to 1,335±112 mg/L.

It can be concluded that the advanced electro-Fenton (AEF) process is an effective process for decolorization and COD reduction of the effluent from biogas chamber. Nevertheless, this treated effluent needs to be further treated to reduce color and COD values to less than 300 ADMI (American Dye Manufacturers Institute) and 120 mg/L to comply with the standard of wastewater discharged regulated by the Pollution Control Department (PCD), Thailand.

Keyword: Hydroxyl radicals; Decolorization; COD reduction; Electro-Fenton; Traditional electro-Fenton (TEF); Advanced electro-Fenton (AEF)

ACKNOWLEDGEMENTS

First, I would like to impress my sincere gratitude to my advisor; Associate Professor Paiboon Sreearunothai, Ph.D (Department of Common and Graduate Studies (CGS), Sirindhorn international institute of technology, Thammasat University) and co-advisor; Korakot Sombatmankhong, Ph.D (National Metal and Materials Technology Center, MTEC), Assistant Professor Winarto Kurniawan, Ph.D. and Professor Hirofumi Hinode, Ph.D (Tokyo Institute of Technology), and Associate Professor Pakorn Opaprakasit, Ph.D (Department of Common and Graduate Studies (CGS), Sirindhorn international institute of technology, Thammasat University) for their valuable help and constant encouragement throughout this thesis. Without their guidance and persistent support, this thesis would not have been possible.

In addition, I am grateful to Assistant Professor Maythee Saisriyoot, Ph.D (Department of Chemical Engineering, Faculty of Engineering, Kasetsart University), for his suggestions and all his help to start up this thesis from impossible to be successful. I am also thank staffs in the laboratory of MTEC (National Metal and Materials Technology Center) who rendered their help during the period of this thesis. I am extremely thankful to Thailand Advanced Institute of Science and Technology-Tokyo Institute of Technology (TAIST-Tokyo Tech), National Science and Technology Development Agency, Thailand and Sirindhorn International Institute of Technology (SIIT), Thammasat University for giving me an opportunity to join the Sustainable Environmental and Engineering Resources of TAIST-Tokyo Tech program (SERE, TAIST-Tokyo tech) which is such a great program providing me several precious experiences during my master's degree life. And I special thank you for wastewater was used in this thesis was provided from Millionaire Suphan Biogreen Power Co., Ltd (Suphanburi, Thailand).

For my friends, thank you a lot to my friends for supporting beside me and fulfilling in every aspect during my master's degree life. Finally, I must express my gratitude to my parents. My parents always give me unconditional support and continuous encouragement. I could not imagine that without their unconditional support and encouragement. I could not this far as I am.

Ms.Preenaphan Tanteerapolchai

TABLE OF CONTENTS

LIST OF TABLES

LIST OF FIGURES

LIST OF SYMBOLS/ABBREVIATIONS

Symbols/Abbreviations	Terms
SIIT	Sirindhorn International Institute of Technology
TU	Thammasat University
TAIST-Tokyo Tech	Thailand Advanced Institute of Science and Technology-Tokyo Institute of Technology
PCD	Pollution Control Department
ADMI	American Dye Manufacturers Institute
COD	Chemical oxygen demand
mg/L	Milligram per liter
AOPs	Advanced oxidation processes
EAOPs	Electrochemical advance oxidation processes
AEF	Advanced electro-Fenton
TEF	Traditional electro-Fenton
AEM	Advanced electrochemical
AEF_0V	Advanced electro-Fenton without applied voltage
•OH	Hydroxyl radical
O_2	Oxygen
$\bullet O_2^-$	Superoxide anion
H_2O_2	Hydrogen peroxide
UV	Ultraviolet
VUV	Vacumm Ultraviolet
O_3	Ozone
TiO_2	Titanium oxide
3D-E	Three dimensional electrochemical
kg/m^3	Kilogram per cubic meter

w/w	Weight by weight
kDa	Kilo-Dalton
ARP	Amadori rearrangement product
HER	Hydrogen evolution reaction
K	Kinetic
g/mol	Gram per mole
V	Volt
W	Watt
EF	Electro-Fenton
Ti/RuO_2-IrO_2	Titanium / ruthenium - oxide iridium oxide
UV-Vis	Ultraviolet visible spectrophotometer
TEF	Tetrafluoroethylene
L/min	Liter per minute
TS	Total solid
BOD_5	Biochemical oxygen demand
RE	Reference electrode
CE	Counter electrode
WE	Working electrode
mM	Millimolar
ED-XRF	Energy Dispersive X-ray Fluorescence
APHA	American Public Health Association
Nm	Nanometer
Mm	Micrometer
DI	Deionized water
C	Current concentration
C_0	Initial concentration

CHAPTER 1

INTRODUCTION

The production of ethanol is one of the major industries in Thailand. It produces a large volume of biogas wastewater which has been increasing with the demand of electricity usage and number of biogas power plants. Some of biogas wastewater is reused as feedstock for a biogas reactor (Janke et al., 2015; Naspolini, Machado, Junior, Freire, & Cammarota, 2017; Reis, Bento, Alves, Carvalho, & Castro, 2019). However, the biogas reactor still generates a large volume of wastewater which has high color value. This wastewater needs to be treated before discharging to the environment.

Most of the treatment plants use the biological process as it is the cheapest technique for removing biodegradable organic pollutants. Nonetheless, treated effluent from the production of ethanol process, particularly from biogas effluent, still contains a very dark brown color. The dark brown color effluent derived from refractory melanoidin from molasses is used as the raw materials (Arimi, Zhang, Götz, & Geissen, 2015) in the production of ethanol. In the past, the color standard for industrial effluent is instinctive. In many cases, it causes the problem to implement and inspect officers since the color is rather subjective and varies from person to person and from time to time. Hence, the existing standard for color is quite impractical. The Pollution Control Department currently intends to revise this color standard to be more scientific and standardized. The color unit in ADMI (American Dye Manufacturers Institute) is proposed since it can be measured accurately and precisely without any sophisticated instrument. The standard values of color and COD (Chemical Oxygen Demand) of wastewater that allows to discharge are 300 ADMI and 120 mg/L of COD (Chemical Oxygen Demand) (Ministry of Industry Thailand, 2019). Once this proposed standard is implemented, it will seriously affect the production of ethanol. As a result, the further treatment for color and COD reduction (tertiary treatment) is needed.

Molasses is considered as a refractory to biodegradation because of melanoidin which has metal sulfate, phenolics, and high molecular weight polymeric as main compounds. These compounds cause the wastewater to have dark color (Olennikov & Tankhaeva, 2012; A. R. Santal & N. P. Singh, 2013).

Melanoidin is antimicrobial, antioxidant, and cytotoxic. These properties make melanoidin intractable to biodegradation and still unaffected by biological treatment processes, a chemical treatment approach is required (Rurián-Henares & Morales, 2008).

One of the most promising chemical treatment processes for the water color treatment is advanced oxidation processes (AOPs), a chemical process (Adina Elena Segneanu, 2013) that produces hydroxyl radical (•OH). Hydroxyl radical has highly potential to oxidize the organic pollutants in wastewater; organic contaminants are transformed into intermediate substances in order to become carbon dioxide eventually. Hydroxyl radicals are very sensitive to reaction. Therefore, they need to be produced and used immediately. The advanced oxidation processes that produce hydroxyl radicals are available in a various forms, such as the Fenton process, electro-Fenton process, ultraviolet combined with hydrogen peroxide (UV/H_2O_2) processes, vacuum ultraviolet with hydrogen peroxide (VUV/H_2O_2) processes, ultraviolet and ozone (O_3/UV) processes, ultraviolet with titanium dioxide (UV/TiO_2) and Vacuum ultraviolet (VUV) processes.

The electro-Fenton process is one of the electrochemical advanced oxidation processes (EAOPs) base on electrochemical methods combined with Fenton reaction. The Fenton reaction can generate powerful hydroxyl radicals (•OH) via the addition of ferrous (Fe^{2+}) reacted with hydrogen peroxide (H_2O_2) which produced by the reduction of the dissolved oxygen on the cathode surface by a transfer pathway of two electrons (Davarnejad & Azizi, 2016; Davarnejad, Mohammadi, & Ismail, 2014; Kourdali, Badis, & Boucherit, 2014; Susree, Asaithambi, Saravanathamizhan, & Matheswaran, 2013) The Fenton reaction can also oxidize most refractory organic pollutants into simple compounds or carbon dioxide (CO_2) and water (H_2O) (Lipczynska-Kochany, 1991). However, this wastewater is difficult to use this traditional wastewater treatment process (electro-Fenton). For characteristics of wastewater needs to be used the advanced process to get the most efficiency on color and COD removal.

Normally, the traditional electro-Fenton (TEF) treatment process uses two electrodes (anode and cathode) which several disadvantages including long mass transfer distance (Kong, Wang, Ma, & Gu, 2006; Xiong, Strunk, Xia, Zhu, & Karlsson, 2001), low electrolytic efficiency and low current efficiency (Can, Yao-Kun, Qing, & Min, 2014). To solve these drawbacks, the three electrodes electrochemical oxidation system as an advanced process has been employed by many researchers. It has been used by

inserting some electrodes between two electrodes in the traditional electro-Fenton (TEF) system to improve wastewater treatment efficiency (Z. Liu, Wang, Li, Xu, & Zhu, 2011; Xiong, He, Karlsson, & Zhu, 2003; Zhao, Sun, Xu, & Ni, 2010) by shortened mass transfer distance. The specific characteristics of inserting electrodes (foam nickel) can produce superoxide anion ($\bullet O_2^-$) to react with hydrogen peroxide (H_2O_2) for generating hydroxyl radical, which will enhance the efficiency of the process.

Therefore, in this thesis electro-Fenton process which inserting foam nickel has been called the advanced electro-Fenton (AEF) process to improve wastewater treatment efficiency to reach the most effective color and COD removal efficiency with are a new and interesting process.

Accordingly, this thesis studies the efficiencies of decolorization and COD reduction of the effluent from the biogas chamber can be effective and get the highest yield by advanced electro-Fenton (AEF) process. The advanced electro-Fenton (AEF) process was investigated to find the optimum condition based on various parameters such as initial pH (2-11), initial ferrous concentration (0.5-9 mM), applied voltage (1.0-4.0V), and reaction time (0-300 minutes) on the efficiencies of decolorization and COD reduction. Moreover, removal efficiencies of the advanced electro-Fenton (AEF) process was compared with the removal efficiencies of advanced electrochemical (AEM) process (by adding foam nickel in the electrochemical process), traditional electro-Fenton (TEF) process, and advanced electro-Fenton process without applied voltage (AEF_0V).

CHAPTER 2

REVIEWS OF LITERATURE

2.1 Ethanol production process

The ethanol production process prepares moved forward impressively over a long time. Firstly, preparation of black trade to generate ethanol from sugar industries (refineries), and numerous plants are started to operate by independent refineries, it was creating ethanol. The production process can be divided into 4 sub-processes (Bergmann, Trichez, Sallet, de Paula e Silva, & Almeida, 2018).

2.1.1 Production process

1) Production of crops (sugarcane and plants), Picking up and hauling. The plant of sugarcane is the one kind of semi-perennial plant so that it is required to edit turn by sorting systematically and preserving the soil systematically. It can generally be utilized for a long time. In cycling, the crops are planted with reusing supplements and including nitrogenated in soil. The plant as a rule gathered each 2 along time from the same field of sugarcanes. These days, there have been done sorting mechanically for speculations from the segment and enactment by burning straw. After the cane was collected, it was cut into bit pieces and transported to plants by trucks within 8 hours to dodge corrupt thin e plants.

2) Taking by remove for operation and juice extraction: In this process, sugarcane passes through a cleaning it arrives once, to wash pollutions including other buildups. The cleaning process has damp or dry; then, the drying process is the most environmentally friendly because it does not use water and does not lead to sucrose misfortune. After that, sugarcane is grounded to smash fiber and extend its thickness from 175 to 450 kg/m^3. The juice extraction is prepared by a crusher (a few plants utilize a dissemination prepare) to discharge sucrose. The processing handle extricates the juice using 4-7 process suits with 3-4 weight of each roller, whereas hot water (around 70 °C) passed through the bagasse to progress extraction surrender. The residual bagasse, with a mugginess of half, is sent to boilers to create high-pressure steam. The steam turbine changes over thermic vitality, either mechanical or electrical energy.

3) In sugar production, the sugarcane was extracted to get juice at the beginning process. The liquid is sieved and clarified by tapping to pollutions to avoid undesired sugar reversal. It is used of chemical compounds in clarification such as sulfate (sulfuric

gas) and liming, treat (soil or water) with a line to reduce acidity, and improve fertility or oxygen levels. The clarification handle produces a slim that is utilized by fertilization within the sugarcane crops. By clarification, the juice is warmed to 105 ‘C to lower microbial defilement and to force the coagulation of colloids and emulsification of oil and wax. At the production of sugar, juice concentration is depending on the elevated temperatures. After taking the sugar from the generation process, it remained sugar, while molasses (or nectar). Which sums of glucose to20%) and sucrose (45% - 60%). Molasses are melded with sugarcane juice (starting must) to deliver ethanol in the sugarcane refineries. This can be indispensable because wholesome juices molasses have inhibited compound for yeast aging. In most of the few plants, it is utilized as a substrate to create ethanol.

4) Fermentative processes: As an explanation of the above sugarcane, extracted and physicochemical medications. Maturation of sugar to ethanol of yeast. The beginning of maturation is melding sugarcane juice or must (molasses and sugarcane juice), in which 18% - 22% (w/w) added to decreasing sugars to convert ethanol suspension. Distinctive sorts of maturation forms have been created over time, such as clump handle, fed-batch handle, and ceaseless preparation fed-batch preparation 70% - 75% ethanol. Refineries are standard strengthen time ordinarily endures for 4-6 hours, and maturation is wrapped up around 10 hours. In group preparation, melded sugar production is stacked and connected to a carbon source (must or sugarcane juice) earlier to expand yeast (saccharomyces cerevisiae). The activated yeast (with 30% of yeast cell) speaks to 25% - 30% of the maturation's overall volume, carried out in tanks of 300-30000 m^3. The way this process is inefficient in ethanol. Therefore, it was not using in the production of ethanol(plants). Sin the method is taking place, there is a contaminant under the condition of oxygen consumption. Still, it was being utilized in the research field, in little distilled in a rapid increase of yeast. Including yeast to aging vat and juice amid persistent maturation handless until a large vat within the fed-batch processing was being achieved in serial aging vats; the must they in them with consistent bolster stream rate in the maturation handle. After aging vat, getting its most extreme volume, fermentation until the entire decrease of the sugar is total, and taking with item by cleaning and sterilizing for the following group. It focuses on the maturation processes, such as supporting the most significant consideration of practical cells, extending the duration of the yeast's duration by substrate elevate degeneration. The fed-batch framework is widely utilized

and utilized in roughly 75% of plants in Brazil's industrialization process to get better ethanol, surrender at the finish of maturation, and be a few contaminations. The fermentation handle process can work for long periods at steady state. The performance of maturation vat doing with a consistent tall volume and streams nourish other. Whereas pulling back juice condition is at the same stream rate of the gulf. Continued stent maturation may be prepared for requires to receive data of microorganism's behavior in the surrounding of its workplace. pH, temperature, substrate concentration, ethanol are essential parameters for this method, and biomass impact the framework efficiency requires a unique method plan. The most significant drawback is the contamination of bacterial for long presentation time due to the nonstop. The coming broth (called wine) has around 6%- 12%(v/v) of liquor within the maturation process. Isolating about 60%-70% of yeast cell by centrifugation from the broth, when the yeast suspension is reused, yeast cream is weakened by treated with water and sulfuric corrosive after 2 hours to decrease yeast degradation after collected wine which is sent to cane areas for nutrient as fertilizer. The hydrated ethanol is dried out of vat where cyclohexane is included to get dehydrated ethanol. It can be created to get dehydrated ethanol in another way, used by that expend less energy.

2.2 Melanoidin

Melanoidin has formed a combination of amino and carbonyl groups from the Maillard reaction. Most parts of the color of melanoidin compound are dark brown (Cardona, Machuca-Martínez, & Marriaga-Cabrales, 2013; España-Gamboa et al., 2017; Parsaee, Kiani Deh Kiani, & Karimi, 2019), its molecular weight is high, nitrogen-containing biopolymers and absorbing light at 405 nm (Langner & Rzeski, 2013). And they are end-products of Maillard reaction during the thermal process of nourishment items, bakery, conservation, distillery industry and sugar industry (A. R. Santal & N. Singh, 2013). Moreover, adverse impact of end-products on nourishment items, the melanoidins carried out as a fundamental part of advantage impacts. They are composed of acidic, polymeric, and negative charged colloids presence of the carboxylic acids and phenolic compounds (Kothandapani & Preetha, 2015).

Their beneficial impacts can consolidate metal cations within the chelation such as Cu^{2+}, Cr^{3+}, Fe^{3+}, Zn^{2+}, Pb^{2+}, etc. to formed complex atoms at that point can be accelerated (A. R. Santal & N. Singh, 2013). In addition, they are antimicrobial properties

(Rufián Henares & Morales, 2007), antioxidant movement (Echavarría Vélez, Pagán, & Ibarz, 2013), antihypertensive (Silván, van de Lagemaat, Olano, & del Castillo, 2006), antiallergenic (Rufián-Henares & Morales, 2007) and tumor growth-inhibiting compounds (Kamei et al., 1998). Poisonous to microorganisms is the antioxidant properties of melanoidin that include in preparation for the treatment of wastewater. Recently, the melanoidins equation from the trial is $C_{17}18H_{26}27O_{10}N$. The atomic weight is between 5-40 kDa (Langner & Rzeski, 2013; A. R. Santal & N. Singh, 2013).

2.2.1 Structure of melanoidin

The melanoidin structure is not known indubitably (Smaniotto, Bertazzo, Comai, & Traldi, 2009). In the other study, melanoidins were prepared by monosaccharide by using carbonyl compounds glucose (D-GLC) together with the amino compounds (glycine). In the Maillard reaction, the carbonyl compound is formed to produce deoxyosones through the Amadori product. Deoxyosones form each other in an aldol-type reaction and produce degradation products of amino-branched sugar. In this occurrence, a, a nucleophilic attack of carbanion in C3 of a 3-deoxyhexosulose happens on the C1 of another deoxyhexosulose. Figure 2.1 shows that the formation of amino acids with unsaturated carbonyl oligodeoxyhexosuloses structure will generate oligodeoxyhexosuloses amine as branched melanoidins with amino compounds. The conceivable melanoidin structure from 3-deoxyhexosuloses in Figure 2.3. This attack pathway on C_2 of a 3-deoxyhexosulose is probable, causing minor changes in the structure. 1-Deoxyhexosuloses, 1-amino-1,4-didesoxyhexosuloses and the ARPs can react with a molecule of deoxyhexosulose to produce the melanoidin skeleton. Even though the melanoidins are various chemicals, a lot of studies present the melanoidins are a negative charge in foods and model systems (Cämmerer, Jalyschko, & Kroh, 2002; Wang, Qian, & Yao, 2011).

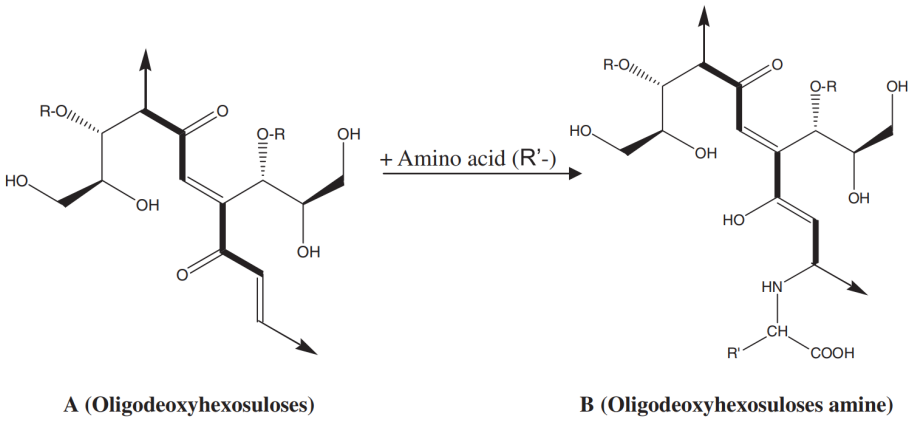

Figure 2.1 The carbohydrate-based of branched melanoidin with amino compounds

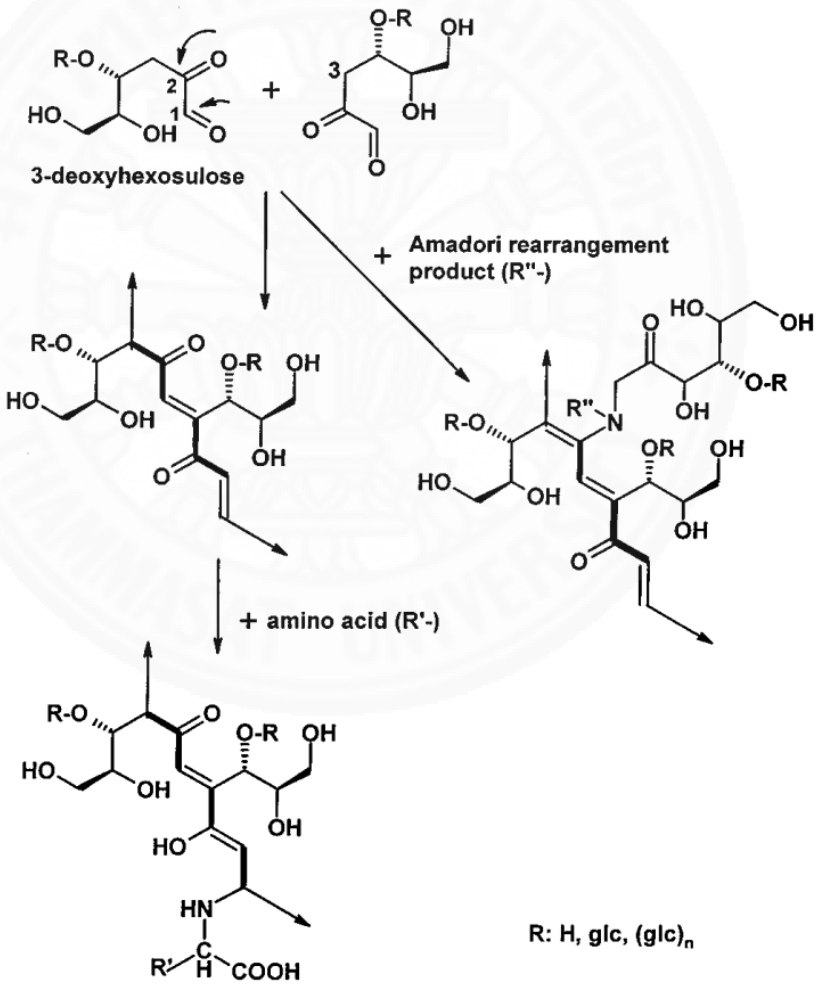

Figure 2.2 Part of possible pathway of melanoidin structure from 3-deoxyhexosulose

2.2.2 Mechanism of the Maillard reaction

Louis Camille Maillard discovered the Maillard reaction in 1912. This reaction is a non-enzymatic browning reaction. Which is complex between the amino group and the carbonyl group of organics and in this reaction, sugar was reduced and close to humic substances in the environment. They are generating colorants, odor and flavor precursors by this reaction for the food process. Maillard reaction products' two pathways are the volatile Maillard reaction products and the non-volatile Maillard reaction products. It can occur at a temperature greater than 50 °C and pH 4-7.

Volatile Maillard reaction products; this study's objectives are to understand the characterization of volatile structure and quantification included with aroma formation. Moreover, coffee flavors can be formed by volatile Maillard reactions in coffee beans processing.

Melanoidins; melanoidins are the end products of the non-volatile Maillard reaction. Melanoidins are brown-colored components, high molecular weight, the combination of sugars and amino acids, low water activity (through reaction) and diets like in honey, cocoa, malt, coffee and bread (E. Koen Bekedam; E. K. Bekedam, 2008).

The melanoidins can be formed on relevant elements such as reaction's types (combination, decomposition, combustion, Redox, etc.), the concentration of reactants, types of substances, optimum pH, high temperature and time, the existence of oxygen, using water, and involving of many kinds of metal ions. And then, the various product can be generated by this reaction from natural gas (e.g., CO_2) to complex polymeric chemicals. These mechanisms composed of three stages are 1) initial reaction of sugar amine condensation between a free amino group and carbonyl group to generate Amadori rearrangement product (ARP). So, the Amadori compounds are the first stable intermediate in the Maillard reaction. It does not happen browning reactions in this initial stage., 2) the consequent decomposition of Amadori compounds involve pH conditions. In condition pH 7 or below. The degradation between dicarbonyl compounds and amino acids will produce aldehydes and α-aminoketones release CO_2. (Rizzi, 1997; Wang et al., 2011), and the last stage is the process of some products condense to form brown colorants and polymers. The amino components react the unsaturated carbonyl structures and form branched melanoidins. And polymerization of reactive intermediates forms of melanoidins. Finally occurring this stage caused by reactions of cyclization, dehydration,

retro aldolization, rearrangement, isomerization, and condensation bring about the brown nitrogenous polymers as melanoidins (Coca et al., 2004; Wang et al., 2011).

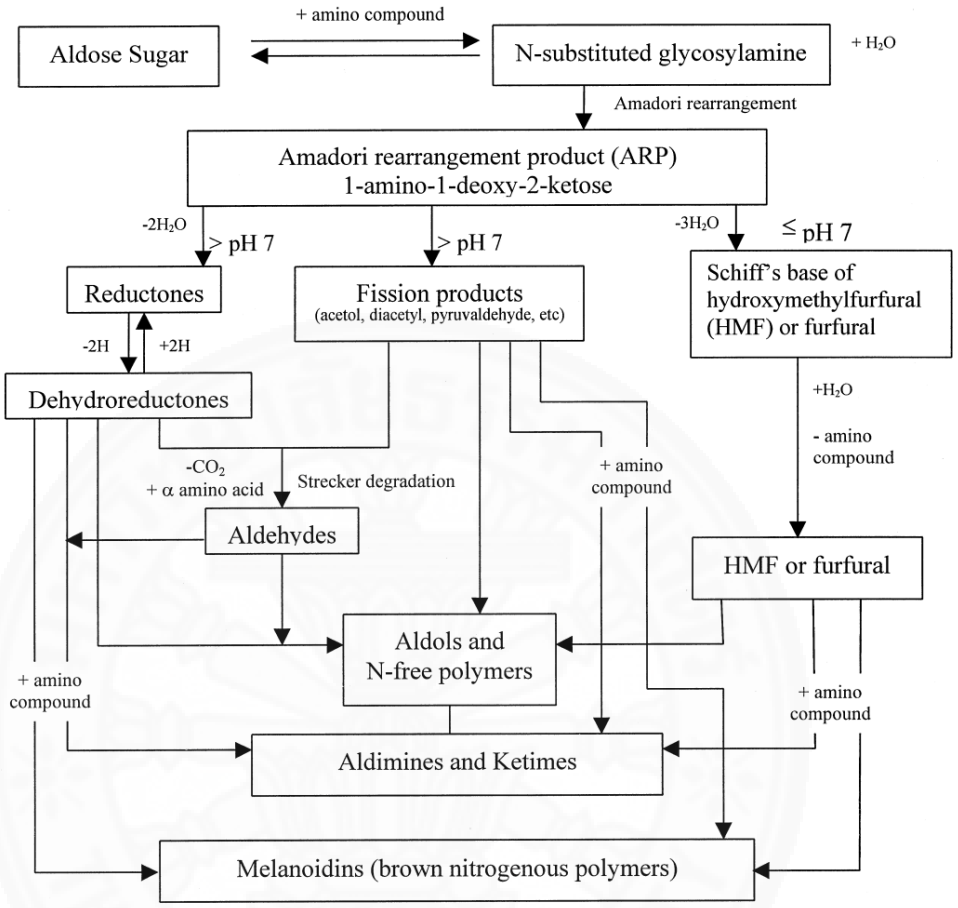

Figure 2.3 Maillard reaction scheme

2.2 Wastewater treatment

The wastewater treatment process consisted of 3 methods physical, biological, and chemical wastewater treatment process. They are used to eliminate the organics or inorganics pollutants in the wastewater. Treatment aims to reduce the contaminants in the wastewater to achieve the acceptable levels or standard values and make water safe before discharge into the natural receiving water (Kant, 14 January 2012). Since melanoidin is antimicrobial, antioxidant, and cytotoxic properties which make them intractable to biodegradation and still unaffected by biological treatment processes, a chemical treatment approach is required.

2.3 Advanced oxidation processes

Advanced oxidation processes (AOPs) (Glaze, Kang, & Chapin, 1987) are the oxidation processes which involve free radicals particularly the hydroxyl radicals (•OH). The organic pollutants can be completely oxidized to carbon dioxide or transformed from converted complexes or organic compounds into biodegradable compounds (Stasinakis, 2008). Hydroxyl radicals (•OH) are non-selective react with electron-rich sites of organic contaminants. The •OH is the most important reactive free radical which can increase the reaction rate up to 1000 times or higher than other oxidants as compared to the oxidation potential in Table 2.1. There are numerous applications of using advanced oxidation processes such as water restoration, wastewater treatment, indirect water reuse, drinking water production, and recently in micro-pollutant control of sewage treatment effluents. This technology will degrade the organic compound in water rather than transfer them into different phrases.

Table 2.1 Comparison of electrochemical oxidation potential of oxidizing agent (Barrera-DÌaz et al., 2017)

Oxidizing agent	Electrochemical Oxidation Potential, (EOP)V
Fluorine	3.06
Hydroxyl Radical (•OH)	2.80
Oxygen (Atomic)	2.42
Ozone	2.08
Hydrogen Peroxide	1.78
Hypochlorite	1.49
Chlorine	1.36
Chlorine Dioxide	1.27
Oxygen (Molecular)	1.23

In general, radicals contain three main parts: (1) Constructing radicals, (2) Reaction of radical, and (3) Radical Recombination. AOPs can be classified by how the radicals were generated. (1) Direct generation from physical based. (2) Generation from adding oxidant to radical. (3) By using a solid catalyst. Many AOPs can include 3

combinations. Furthermore, the classification can be used as the energy type to classify radicals such as electrochemical, temperature, etc.

Generally, there are many types of AOPs such as photocatalysis (UV/H_2O_2, UV/TiO_2), Fenton and Fenton-like processes (H_2O_2/Fe^{2+}), ozonation (UV/O_3), electrochemical processes, and vacuum ultraviolet (VUV).

2.4 Fenton process

Fenton's reagent was discovered in 1894 by its inventor Henry J. Fenton, but its application as an oxidizing process for destroying toxic organics was applied in the rate 1960s (Huang, Dong, & Tang, 1993). Fenton reaction is one kind of AOPs used to generate hydroxyl radicals (•OH) for the degradation of pollutants. This reaction involves chemical reagents called "Fenton's reagent", which are the combination of hydrogen peroxide (H_2O_2) and a ferrous iron (Fe^{2+}). Fenton's reagent is an effective and simple oxidant of various types of organic contaminants (Gawande, 2015, 2016; Mishra et al., 2017).

2.4.1 Hydrogen peroxide

Hydrogen peroxide (H_2O_2) is an aqueous solution with a clear, colorless, water-like appearance and can be mixed with water in any proportion. It is miscible with cold water and is soluble in alcohol and ether. At high concentrations has slightly pungent or acidic odor. The chemical formula is H_2O_2 and it has molecular weight of 34.015 g/mole and is non-flammable at any concentrations. Hydrogen peroxide is a diprotic acid with K_{A1} and K_{A2} equal to $10^{-11.8}$ and $<10^{-14}$, respectively.

Although pure H_2O_2 is relatively stable, it significantly decomposed into water and oxygen when heated above about 60 °C or in the presence of reducing agents. Aqueous solution of H_2O_2 is mainly used for oxidation reactions, including bleaching process, chemical synthesis, and for water and wastewater treatment. In drinking water purification, Hydrogen peroxide is used to pre-oxidize organic constituents and to eliminate iron and manganese ions. In addition, H_2O_2 can also provide oxygen to microorganism in biological treatment facilities and in the bioremediation of polluted sites by dissociation into oxygen and water. It can be used to control the excessive growth of biofilm from the biological treatment process as a disinfection reagent. Due to the fact that the concentration of oxygen is usually limits the biodegradation of organic pollutants

in presence. To enhance the biodegradation activities, many applications using H_2O_2 injection into the subsurface have been recently applied. H_2O_2 decomposition into water and oxygen may be directed toward by enzymatic and non-enzymatic routes.

Hydrogen peroxide also catalytically decomposes in the presence of numerous catalysts, e.g., most transition-metal ions such as Fe^{2+}, Cu^{+}, Cu^{+}, Cu^{+}, or UV irradiation via different route to form a highly oxidative $OH^{\bullet}$.

2.4.2 Ferrous

Iron (Fe) is the most abundant element on Earth and is the cheapest and the most important of all metals. Iron is used to manufacture steel and other alloys important in construction and manufacturing. It also plays a vital role in the functioning of living organisms by transporting oxygen in blood via the hemoglobin molecule (an iron complex organic compound). Its oxidation number varies from -2 to +6; however, most general states typically found in the environment are ferrous (Fe^{2+}) and ferric (Fe^{3+}). Iron exists in the ferrous state under reducing conditions such as those in anaerobic environment. Ferrous iron will be rapidly oxidized to ferric state when exposed to oxidizing agents; hence, it is not stable in the atmospheric environment where oxidative oxygen gas is present (21% by volume)

As mentioned previously, several transition-metal ions can catalyze the decomposition of H_2O_2 to form •OH, Fe^{2+} is the most preferred and environmentally friendly among all transition-metal catalysts. Iron (II) sulfate is the most common form of ferrous salt commercially available in the market and can be found in various states of hydration; however, the heptahydrate or so called “green vitriol or copperas” ($FeSO_4.7H_2O$) is the most common. This greenish crystalline compound is used as a pigment, fertilizer, medicine in the treatment of iron deficiency, coagulant for the coagulation process, and catalyst in the Fenton process.

2.4.3 Hydroxyl radicals

Hydroxyl radicals (•OH) is extremely reactive, short-lived, and non-selective transient species. It is a strong oxidant with very high oxidizing capacity equaling 2.80 V (Barrera-DÌaz et al., 2017; Masten & Davies, 1994). Table 2.2 shows the oxidation potential of •OH compared to other oxidants. It can be seen that •OH is the second most potent oxidant, which is inferior only to fluorine. Hydroxyl radicals can decompose the

organic compounds relatively unselective (Metcalf & Eddy et al., 2003) with the rate constants ranging from 10^9-10^{10} $M^{-1}s^{-1}$ (Buxton, Greenstock, Helman, & Ross, 1988).

Hydroxyl radicals are generated among various AOPs in the reaction mixture and have been used for achieving the treatment of a myriad of contaminated waters and industrial wastewaters. Hydroxyl radicals can react in aqueous solution by different types of reaction (Equations (2.1) to (2.4)) depending on target compounds, wastewater composition, and environment conditions (Hoigne, 1998).

Electro transfer reaction: $\bullet OH + M^n \rightarrow M^{n+1} + (OH^-)_{(aq)}$ (2.1)

Hydrogen abstraction: $\bullet OH + R\text{-}H \rightarrow R^\bullet + H_2O$ (2.2)

Electrophilic addition: $\bullet OH + R_2C{=}CR_2 \rightarrow {}^\bullet CR_2\text{-}C(OH)R_2$ (2.3)

Radical interaction: $\bullet OH + OH^\bullet \rightarrow H_2O_2$ (2.4)

For complex or large aliphatic hydrocarbons, $OH^\bullet$ will oxidize via electrophilic addition to forming carbon-center radicals which immediately further react in a biomolecular reaction with dissolved oxygen to produce peroxide radicals and sequentially stable oxidation products. On the other hand, c tends to react with small aliphatic compounds by hydrogen abstraction mean in which carbon dioxide can be formed as the final product (complete mineralization). The oxidation of aromatic compounds by •OH is more complicated than aliphatic hydrocarbons and could involve hydrogen abstraction, electrophilic addition, and radical interaction. Direct electron transfer normally occurs with inorganic pollutants. In addition, •OH itself can react with another •OH to combine or to disproportionate to form a stable product (Peres, Beltrán, & Domínguez, 2004).

2.4.4 Fenton reaction

Fenton process and its modified versions are being increasingly used in the treatment of contaminated water and soil. The conventional “dark” Fenton process involves the use of an oxidizing agent (usually H_2O_2) and a catalyst (usually Fe^{2+}) to generate highly reactive •OH. Once the Fenton’s reagent is combined together, its sequential reactions are very complicated but well specified as shown in Equations (2.5) to (2.16) (Chen et al., 2001; Pignatello, 1992).

$Fe^{2+} + H_2O_2 \rightarrow Fe^{3+} + \bullet OH + OH^-$; $k_1 = 76\ M^{-1}s^{-1}$ (2.5)

$H_2O_2 \leftrightarrow HO_2^- + H^+$; $K_2 = 1.59x10^{-2}\ M$ (2.6)

$Fe^{3+} + H_2O_2 \rightarrow Fe^{2+} + HO_2\bullet$; $k_3 = 0.02\ M^{-1}s^{-1}$ (2.7)

$HO_2\bullet \leftrightarrow \bullet O_2^- + H^+$; $K_4 = 1.6x10^{-5}\ M$ (2.8)

$Fe^{2+} + \bullet OH \rightarrow Fe^{3+} + OH^-$; $k_5 = 4.3x10^6\ M^{-1}s^{-1}$ (2.9)

$Fe^{2+} + \bullet O_2^- \rightarrow Fe^{3+} + \bullet O_2^-$; $k_6 = 1x10^7\ M^{-1}s^{-1}$ (2.10)

$Fe^{2+} + HO_2\bullet \rightarrow Fe^{3+} + HO_2$; $k_7 = 1.2x10^6\ M^{-1}s^{-1}$ (2.11)

$H_2O_2 + \bullet OH \rightarrow HO_2\bullet + H_2O$; $k_8 = 2.7x10^7\ M^{-1}s^{-1}$ (2.12)

$HO_2\bullet + HO_2\bullet \rightarrow H_2O_2 + O_2$; $k_9 = 8.3x10^5\ M^{-1}s^{-1}$ (2.13)

$\bullet OH + \bullet OH \rightarrow H_2O_2$; $k_{10} = 5.3x10^9\ M^{-1}s^{-1}$ (2.14)

$RH + \bullet OH \rightarrow RH\bullet + OH^- \rightarrow\rightarrow\rightarrow$ product or $CO_2 + H_2O$ (2.15)

$Fe^{3+} + 3OH^- \rightarrow Fe(OH)_{3(s)}$; $K_{sp} = 4x10^{-38}$ (2.16)

Although Fe^{2+} is acting as a catalyst in the Fenton reaction series, it can be seen that the consumption rate of Fe^{2+} in Equation (2.5) is almost 3,800 times faster than the regeneration rate of Fe^{2+} from Fe^{3+} in Equation (2.7). As a result, the pollutant degradation in Fenton process typically proceeds in two sequential steps. In the first step, the pollutant disappears rapidly under sufficient Fe^{2+} leading to the •OH excessive environment whereas, in the slower second step, the oxidation rate of the contaminant is controlled by Equation (2.7) which is known as the "Fenton-like process" (Lunar, Sicilia, Rubio, Pérez-Bendito, & Nickel, 2000). After treatment with the Fenton process, the mixture is typically neutralized to comply with the effluent standard and the ferric hydroxide will precipitate out as illustrated in Equation (2.16). This ferric hydroxide sludge will cause a burden for further separation and disposal which is a significant drawback for the ordinary Fenton process.

2.5 Advanced electro-Fenton process

The traditional electro-Fenton (TEF) process is a process used in the Fenton process combined with the electrochemical process to treat wastewater by generating hydroxyl radicals to oxidize the pollutants in the wastewater. Fenton reaction, which happens between ferrous ion and hydrogen peroxide to produce hydroxyl radicals according to the Equation (2.5).

The electro-Fenton process is the process that led to the electrochemical process applied together, which results in the ability to create hydrogen peroxide from electrodes and the addition of ferrous ion into solution. The electricity is released into electrodes that will cause corrosion, and discharge ions are coming out to react to cause the organic matter in the wastewater is oxidized and precipitated by the electro-Fenton. The traditional electro-Fenton (TEF) process is electrolysis that can produce hydrogen peroxide by using electrodes made from graphite as the cathode. The cathode had the reduction reaction and dissolved oxygen on the surface, and when the reaction is produced with $2H^+$, the hydrogen peroxide is generated. The anode had the oxidation reaction and loss of 2 electrons of water. The product is $\frac{1}{2}$ O_2 and $2H^+$ by the overall reaction of hydroxyl radicals, as shown in Equations (2.17) to (2.19).

Hence, in this basic mechanism, the start step is the step of production of •OH by the response of hydrogen as per the Equation (2.5). At that point, most organic compounds can react quickly and non-selective with these hydroxyl radicals and cause their chemical breakdown:

$$B + OH^- \rightarrow B_{oxid} \quad (2.17)$$

Though, hydroxyl radicals ($OH^\bullet$) may be scavenged by the reaction with the hydrogen peroxide present or with another ferrous (Fe^{2+}) molecule:

$$H_2O_2 + \bullet OH \rightarrow HO_2^\bullet + H_2O; \quad (2.18)$$

$$HO_2^\bullet + HO_2^\bullet \rightarrow H_2O_2 + O_2; \quad (2.19)$$

$$Fe^{2+} + \bullet OH \rightarrow Fe^{3+} + OH^-; \quad (2.20)$$

At last, the reaction between H_2O_2 especially hydroxyl radicals and ferric (Fe^{3+}), with the recovery of ferrous (Fe^{2+}) (Bautista, Mohedano, Gilarranz, Casas, & Rodriguez,

2007). So, the significant effect of the process performance was considered by the hydrogen peroxide concentration. The initiator producing of this process is not only hydrogen peroxide but also the •OH scavenger if it presents in excess.

In the electro-Fenton process, H_2O_2 is formed by the reduction of the dissolved oxygen on the cathode surface (Equation (2.21)). H_2O_2 can then react with the additional added Fe^{2+} to produce •OH (Equation (2.22)), and this reaction is Fenton's reaction.

$$O_2 + 2H^+ + 2e^- \rightarrow H_2O_2 \quad (2.21)$$

$$Fe^{2+} + H_2O_2 \rightarrow Fe^{3+} + \bullet OH + OH^- \quad (2.22)$$

$$Fe^{3+} + e^- \rightarrow Fe^{2+} \quad (2.23)$$

Fluorine is the highest oxidation potential, while hydroxyl radicals are continuously following. However, fluorine produced high toxicity, so the hydroxyl radicals would be considered by reacting entirely and rapidly with most organic pollutants to degrade the most organic pollutants. Furthermore, the regeneration of Fe^{2+} from the reduction of Fe^{3+} at the cathode (Equation (2.23)) is important for the electro-Fenton process (M. Oturan, Peiroten, Chartrin, & Acher, 2000; M. A. Oturan, Oturan, Lahitte, & Trevin, 2001; Pirvu, Brillas, Radovici, & Banu, 2004). The result of reactions in Equations (2.21) to (2.23) gives the global reaction that happens in the cathodic compartment (Equation (2.24)). In the anodic case, the reaction that occurs is simply the oxidation of water (Equation (2.25)). The overall response (Equation (2.26)) happening in the electrolysis cell and leading to the production of hydroxyl radicals indicates the catalytic character of elector-Fenton process. Therefore, the reagents for •OH are oxygen and energy from the electrical generator (M. A. Oturan & Pinson, 1995).

Cathode:

$$O_2 + 3H^+ + 3e^- \rightarrow H_2O + \bullet OH \quad (2.24)$$

Anode:

$$H_2O \rightarrow \frac{1}{2} O_2 + 2H^+ + 2e^- \quad (2.25)$$

Redox:

$$\frac{1}{2}O_2 + H_2O \rightarrow 2\ \bullet OH \quad (2.26)$$

The outstanding performance of electro-Fenton processes with inserting foam nickel as the advanced electro-Fenton (AEF) process could enhance the production of hydroxyl radicals, which can be generated by two pathways.

First, the addition of ferrous (Fe^{2+}) can react with hydrogen peroxide (H_2O_2) produced from the reduction of the dissolved oxygen on the cathode surface by a transfer pathway of two electrons as shown in Equation (2.27) to produced hydroxyl radicals in Equation (2.28).

$$O_2 + 2H^+ + 2e^- \rightarrow H_2O_2 \quad (2.27)$$

$$Fe^{2+} + H_2O_2 \rightarrow Fe^{3+} + \bullet OH + OH^- \quad (2.28)$$

Another pathway of hydroxyl radicals (•OH) is generated by the Haber-Weiss reaction as shown in Equation (2.29). The Haber-Weiss reaction create $\bullet O_2^-$ from the dissolved oxygen which adsorbed on the surface of foam nickel and hydrogen peroxide (H_2O_2) from the superoxide anion ($\bullet O_2^-$) react with one electron transfer pathway according to Equations (2.30) and (2.31).

$$\bullet O_2^- + H_2O_2 + 2H^+ \rightarrow O_2 + \bullet OH + OH^- \quad (2.29)$$

$$Ni + 2O_2 \rightarrow Ni^{2+} + 2\bullet O_2^- \quad (2.30)$$

$$\bullet O_2^- + e^- + 2H^+ \rightarrow H_2O_2 \quad (2.31)$$

2.5.1 Electrodes

Electrodes are the component of each electric half-cell. Electrodes act as a conductor of electricity connected between electrolytes and measuring of the electrical signal. It is divided into 3 types 1. reactivity electrodes (Active Electrodes), 2. non-reactivity electrodes (Inert Electrodes), and 3. gas electrodes. The electrodes were used in this study is Ti/RuO_2-IrO_2, graphite felt, and foam nickel because of their characteristics to enhance the efficiency of wastewater treatment.

1) Titanium is a transition metal, the color looks like silver, high melting point and boiling point, hardness, and toughness. Typically titanium is relatively inert, it withstands dry chlorine gas, but if the temperature is very high temperature (than 500 °C) it can react forcefully with a metal compound. Then have the covalent compound such as TiO_2, $TiCl_4$, etc. Hydroxide and hydrogen were generated by titanium reacted with water. The oxidation numbers of titanium are +2, +3, and +4 which is stabilized at +4. Titanium was used as electrodes in the electrolytic cell and it does not make other metal cause corrosion during electrolysis reaction. Moreover, at the negative electrode found to have many heavy metals, sediment does not occur in the solution. It is also high efficiency in high melting point and boiling point in normal state. For this study, the Ti/RuO_2-IrO_2 was used as anode electrodes for wastewater treatment, the reasons supported by the information as shown in Table 2.2.

Table 2.2 Treatment of industrial wastewater with electro-Fenton and peroxicoagulation (Barrera-DÌaz et al., 2017)

Type of wastewater	Electrode/ electrochemical cell	Operation conditions	Efficiency /main results obtained in terms of treatability
		Electro-Fenton	
Landfill leachate	Sacrificial iron anode	pH 3.0	72 % COD removal in 20 minutes
Olive oil mill wastewater	Sacrificial iron anode	pH 3.0	Mineralization in 9 h at 200 mA
Flame retardant industry wastewater	Sacrificial iron anode	pH 1.5	99.9 removal of P-compunds
Petrochemical industry wastewater	Sacrificial iron anode		94% COD removal in 5 h
Slaughterhouse wastewater	Sacrificial iron anode	pH 7.8, 6% H_2O_2, current density 20 mA cm^{-2}	81% COD removal, 91% turbidity removal
Dairy industry wastewater	Iron anode and aluminum cathode	pH 6.5-7.0, current density 15 mA cm^{-2}, external H_2O_2 addition 3x 1000 mg L^{-1}	75% COD removal, 91% turbidity removal
Landfill leachate	Anode (Ti/RuO_2–IrO_2)	pH 3, 0.34 mol/L H_2O_2, 0.028 mol/L Fe^{2+}, current 2 A	80% COD removal
Alcohol distillery wastewater	iron electrodes	pH 4, current density 60 mA cm^{-2}, 0.3 M Na_2SO_4 and 60.000 mg L^{-1} H_2O_2	COD removal efficiency of 92.6% TOC removal efficiency of 88.7%
Photographic processing wastewater	BDD anode, carbon felt cathode. Single compartment cylindrical cell	pH 3, current 300 mA	90% TOC removal
Photographic processing wastewater	Pt anode, carbon felt cathode. Single compartment cylindrical cell	pH 3, current 300 mA	30% TOC removal
Wastewater	Platinized titanium electrode	Current density 340 mA cm^{-2}, ratio Fenton reagent to H_2O_2 1:20	100% COD and NH4+ removal after 4 h

2) Graphite is an allotrope of carbon. The common name is called “Plumbago” or black pencil ore. It has thin solid crystalline, color is dark gray or black, and can use as a conductor of heat and electricity in the parallel direction to the plane of atoms. However, in a direction perpendicular to the plane of atomic will be less of conductivity. Graphite atoms are arranged in a planar layer. Carbon atoms in each layer are located at the corners of the regular hexagon shaped. The adhesion between the plane was not chained together by covalent bond but chained by van der waals force. The distance between the carbon atoms is 1.415 Angstrom, which is short enough to allow the carbon atom attached to the other atoms by multiple bonds. The graphite was used as the pencil lead, crucible, lubricants, batteries, light arc, etc. The working electrode is was represented as cathode. The cathode (working electrode) was widely applied in the wastewater is activated carbon fiber or graphite felt because it had a large surface; it can increase the production of H_2O_2 from oxygen reduction (Kong et al., 2006). For this study, the graphite was used as electrodes for wastewater treatment. The graphite felt is like fiber material so, they have many porosities for absorbed pollutant in theirs. Thus, graphite felt was used in this study to increase the efficiency of the wastewater treatment process.

3) Foam nickel is an absorbable material with many applications. The characteristic is very high porosity, typically 75-95% is void space. Examples of applications such as thermal insulation in Ceramic foam form, acoustic insulation, adsorption of environmental pollutants, and perform as the catalyst reaction substrate. Foam nickel was used as insertion electrode and the mechanism was shown in Equations (2.32) to (2.33).

$$Ni + 2O_2 \rightarrow Ni^{2+} + 2{\bullet}O_2^- \quad (2.32)$$

$${\bullet}O_2^- + {\bullet}O_2^- + 2H^+ \rightarrow H_2O_2 + O_2 \quad (2.33)$$

Foam nickel can enhance degradation efficiency by more hydroxyl radicals generated when foam nickel was added in the process (Nishikimi, Appaji, & Yagi, 1972). Because foam nickel had dissolved oxygen adsorbed on the surface. Then, foam nickel electrodes could activate molecular oxygen to produce $\bullet O_2^-$ via a single-electron transfer pathway to subsequently generate more H_2O_2 and hydroxyl radicals (W. Liu, Ai, & Zhang, 2012). In various conditions following Table 2.3:

Table 2.3 Conditions of experiment to investigated the effectiveness of foam nickel

Conditions	Electricity	Foam nickel	Ferrous
1	/	/	/
2	/	/	x
3	/	x	/
4	x	/	/

Condition 1: Advanced electro-Fenton (AEF) process

$$Ni + 2O_2 \rightarrow Ni^{2+} + 2{\bullet}O_2^- \quad (2.34)$$

$$O_2 + e^- \rightarrow {\bullet}O_2^- \quad (2.35)$$

$$O_2 + 2H^+ + 2e^- \rightarrow H_2O_2 \quad (2.36)$$

$${\bullet}O_2^- + {\bullet}O_2^- + 2H^+ \rightarrow H_2O_2 + O_2 \quad (2.37)$$

$${\bullet}O_2^- + H_2O_2 + 2H^+ \rightarrow O_2 + {\bullet}OH + OH^- \text{ ; Haber-Weiss reaction} \quad (2.38)$$

$$Fe^{2+} + H_2O_2 \rightarrow Fe^{3+} + {\bullet}OH + OH^- \quad (2.39)$$

Condition 2: Advanced electrochemical (AEM) process

$$Ni + 2O_2 \rightarrow Ni^{2+} + 2{\bullet}O_2^- \quad (2.40)$$

$$O_2 + e^- \rightarrow {\bullet}O_2^- \quad (2.41)$$

$$O_2 + 2H^+ + 2e^- \rightarrow H_2O_2 \quad (2.42)$$

$${\bullet}O_2^- + {\bullet}O_2^- + 2H^+ \rightarrow H_2O_2 + O_2 \quad (2.43)$$

$${\bullet}O_2^- + H_2O_2 + 2H^+ \rightarrow O_2 + {\bullet}OH + OH^- \text{ ; Haber-Weiss reaction} \quad (2.44)$$

Condition 3: Traditional electro-Fenton (TEF) process

$$O_2 + e^- \rightarrow \bullet O_2^- \quad (2.45)$$

$$\bullet O_2^- + \bullet O_2^- + 2H^+ \rightarrow H_2O_2 + O_2 \quad (2.46)$$

$$O_2 + 2H^+ + 2e^- \rightarrow H_2O_2 \quad (2.47)$$

$$\bullet O_2^- + H_2O_2 + 2H^+ \rightarrow O_2 + \bullet OH + OH^- \text{ ; Haber-Weiss reaction} \quad (2.48)$$

$$Fe^{2+} + H_2O_2 \rightarrow Fe^{3+} + \bullet OH + OH^- \quad (2.49)$$

Condition 4: Advanced electro-Fenton process without applied voltage (AEF_0V)

$$Ni + 2O_2 \rightarrow Ni^{2+} + 2\bullet O_2^- \quad (2.50)$$

$$\bullet O_2^- + \bullet O_2^- + 2H^+ \rightarrow H_2O_2 + O_2 \quad (2.51)$$

$$\bullet O_2^- + H_2O_2 + 2H^+ \rightarrow O_2 + \bullet OH + OH^- \text{ ; Haber-Weiss reaction} \quad (2.52)$$

$$Fe^{2+} + H_2O_2 \rightarrow Fe^{3+} + \bullet OH + OH^- \quad (2.53)$$

4) Aluminium has white color, shiny, lightweight, and high conductivity. It can be easily reacted to certain types of acids and alkalis. It is very rigid, as it can be hard to cracks. Aluminum can be considered as active interaction with other non-metals. Its oxidation number is +3 compounds, usually covalent compounds. Once in the water, Al^{3+} produced hydration and hydrolysis, salt, sulfate, nitrate, and aluminum halides. Using aluminium as electrodes in electrolytic cells when the electrolysis reaction has happened electrolyte reaction causes the aluminum to be corrosive and will be solubility in solution. Therefore, there may have a lot of colloids in solution.

5) Steel is a heavy metal with a high boiling point, melting point, and have medium reactivity. The steel compounds have an oxidation + 2 and + 3 and have some high oxidation numbers but are unstable. There are very strong oxidize if left it in the air with moisture, it would become brown color on the surface is called “rust”. The steel can react with almost of non-metal when it is slightly hotter. However, it does not react with nitrogen when it is in a solution. Steel is regularly in the form of Fe^{2+} and Fe^{3+}. Steel with

a + 2 oxidative number is very stable and can cause salt with stable anion. The anhydrous Fe^{2+} is colorless, but if there has water or in a solution, the light green is caused by ion of $(Fe(H_2O)_6)^{2+}$. The solution contained Fe^{2+} was oxidized by the air to produce Fe^{3+}. Fe^{3+} in the solution of water as hydrated ion because the Fe^{3+} has a small ion and large ionic size thus that showing the acidic properties. Therefore, both the Fe^{2+} and Fe^{3+} can react with the substance that gives electrons and a complex substance. Using steel as electrodes in electrolytic cells when an electrolysis reaction has occurred on the surface of the anode electrode. The corrosion will happen because of the discharging of an electron with Fe^{2+} at the cathode electrode, hydroxide ion is generated which makes the high pH. The steel made from the anode electrodes can precipitate in hydroxide form, such as $Fe(OH)_2$. So, the amount of precipitation depends on the concentration of hydroxide is produced from the cathode electrode and the pH. Hence it needs to replace the steel sheet in the electrolyte cells when used for a while. The steel is easy to find and cheaper price. And steel is so famous for use in wastewater treatment.

6) Stainless steel is classified as a type of alloy steel. The main alloying element is chromium which about more than 11%. The film of chromium oxide (Cr_2O_3) is produced by chromium elements in steel which stable at the surface of the steel. This film is shiny and prevents the oxidation in steel which inside stainless steel for providing the corrosion-resistant.

7) Platinum has white color, several oxidation numbers ranging from +2 to + 8, but the often used is + 2 to + 4 with a boiling point of 3,827 °C and a melting point of 1,770 °C. Besides, the compound of platinum is often unstable when put heat to disintegrate into metal. Therefore, these metals are found in the form of independent elements in nature. In addition, it can associate with other elements such as copper, silver, and gold. There has the disadvantage of very rare to buy, so it is hard to use in the wastewater treatment process because of its very expensive (M. Oturan et al., 2000; Pirvu et al., 2004). Nevertheless, it has a high thermal and electrical conductivity. There is an inert reaction, so it is useful to made electrodes, fire-resistant electrodes, and containers for high-temperature applications or high corrosion-resistant.

2.7 Literature reviews

Liu et al. (2014) investigated integrated processes for higher rhodamine B (RhB) wastewaters. In this work, using the three-dimensional electro-Fenton process for wastewater treatment with using electrodes of Ti/RuO_2-IrO_2, Graphite Felt, and Nickle Foam were used as anode, cathode, and support electrodes, respectively. This electro-Fenton process was optimized under optimum conditions pH value was 6.2, reaction time of 30 min, 2.0 Voltage, and Fe^{2+} 3 mmol/L concentration was applied. About 99% could degrade of RhB with used foam nickel as particle electrodes that higher degradation efficiency than other particle electrodes such as foam titanium and iron shaving (W. Liu et al., 2012).

Zhang et al. (2006) investigated the removal of COD from landfill leachate using the Electro-Fenton method was carried out in a batch reactor. The initial chemical oxygen demand (COD) of wastewater is 5,000 mg/L. The variables are considered included distance between electrodes, reaction time, intensity of current, ratio hydrogen peroxide and ferrous ion, and the amount of hydrogen peroxide and Fenton reagent. From this study found that the use of the effective in reducing the size of organic molecules is very fast within first 30 minutes and then slow down and finish within 75 minutes. The distance between the electrodes is effective in COD removal. The results found that COD removal efficiencies increased with the increasing of intensity of current, but if it further increases of current would reduce removal efficiency. The organic matter removal efficiencies increased with the increasing of ferrous ion and hydrogen peroxide concentration by the ratio of 0.038 mol/L. Therefore, the results found that only the electrochemical process cannot decrease the reduction of COD. As well as the Fenton process also cannot reduce the COD (Zhang, Zhang, & Zhou, 2006).

Atmaca et al. (2009) Electro-Fenton method was used as the wastewater treatment process for landfill leachate in Siavas, Turkey. The steel in dimension 4x5 cm was used as electrode in this study and connected in the parallel direction in reactor. The results showed that the initial pH value had an effect on the treatment process. The reaction between pH 2-4 is appropriate of this process. On the other hand, the efficiency was reduced by about more than 50% by increased the pH. So, the high removal efficiency was 3-3.5 of pH value. And the results showed that when the removal efficiency of sodium nitrate and phosphate increased with the increasing of current. The appropriate initial concentration can improve treatment efficiency. For conclusion, current equal to 2

A and 20 minutes of retention time. Results showed removal efficiency of bout 72%, 90%, 26%, and 87% for COD removal, color reduction, NH_3-NO^-_3 removal, and phosphate-phosphorus, respectively (Barrera-DÌaz et al., 2017).

CHAPTER 3

METHODOLOGY

3.1 Materials, chemicals and reactor construction

3.1.1 Materials

1) Electrodes
   - Ti/RuO_2-IrO_2 electrode was used as the anode with
   - Graphite Felt electrode was used as the cathode
   - Foam Nickel electrode was used as the support electrode
2) Compact design potentiostat/ galvanostat instrument, Metrohm, PGSTAT 204
3) Magnetic stirrer, IKA C-MAG HS 7
4) Aquarium air pump, 6.5 L/min, 6.0 W, 110/220 V, and 50/60 Hz, Hailea, ACO-9905
5) Micro Energy Disperse X-ray Fluorescence Spectrometer, Orbis PC
6) pH meter, Okaton waterproof, pHTestr 30
7) UV-Vis spectrophotometer, Merck, Pharo 300
8) Erlenmeyer flask
9) Volumetric flask
10) Cylinder
11) Burette
12) Micro pipette (Autopipette)
13) Digestion vessels 16 x 100 mm with the tube caps was made from Tetrafluoroethylene (TEF)
14) Block heater, Spectroquant TR 420 thermoheater (150 ± 2 °C)

3.1.2 Chemicals

All chemical reagents used in this thesis work were analytical reagent grade.

1) Wastewater was used in this thesis was obtained from Millionaire Suphan Biogreen Power Co., Ltd (Suphanburi, Thailand).
2) Sulfuric Acid (H_2SO_4), LOBA Chemie Pvt. Ltd.
3) Potassium Dichromate ($K_2Cr_2O_7$), LOBA Chemie Pvt. Ltd.

4) Ammonium Iron (II) Sulfate Hexahydrate (Fe(NH4)2(SO4)2.6H2O), Daejung
5) Silver Sulfate (Ag_2SO_4), Poch
6) Mercury (II) Sulfate ($HgSO_4$), Carlo Erba
7) Ferroin Indicator Solution 0.025M, LOBA Chemie Pvt. Ltd.
8) Potassium Hydrogen Phthalate (KHP, $C_8H_5KO_4$), Daejung
9) Sulfamic Acid ($HOSO_2NH_2$), Daejung
10) Potassium Iodide (KI), LOBA Chemie Pvt. Ltd.
11) Ammonium Molybdate ($(NH_4)_6 Mo_7O_{24}.4H_2O$), LOBA Chemie Pvt. Ltd.
12) Ammonium Hydroxide Solution (NH_4OH), LOBA Chemie Pvt. Ltd.
13) Ammonium Nitrate (NH_4NO_3), Scitrader
14) Starch Soluble (Ex Potato), LOBA Chemie Pvt. Ltd.
15) Sodium Thiosulfate Standard Solution 0.01M, LOBA Chemie Pvt. Ltd.
16) Iron (II) Sulfate ($FeSO_4.7H_2O$), LOBA Chemie Pvt. Ltd.
17) Sodium Sulfate Anhydrous (Na_2SO_4), Fisher
18) 1,10-Phenanthroline Monohydrate ($C_{12}H_8N_2.H_2O$), Sigma Aldrich
19) Acetic Glacial Acid (CH_3COOH), LOBA Chemie Pvt. Ltd.
20) Hydrochloric Acid 0.1M (HCl), Fisher
21) Hydroxylammonium Chloride ($NH_2OH.HCl$), LOBA Chemie Pvt. Ltd.
22) Ammonium Acetate ($NH_4C_2H_3O_2$), LOBA Chemie Pvt. Ltd.
23) Potassium Permanganate ($KMnO_4$), Honeywell Fluka
24) Sodium Hydroxide (NaOH), LOBA Chemie Pvt. Ltd.
25) Sylgard 184 Silicone Elastomer, Dow Corning

3.1.3 Advanced electro-Fenton (AEF) reactor construction

The advanced electro-Fenton (AEF) process was conducted in a rectangular polymethyl methacrylate (PMMA or ACRYLIC) reactor with dimensions of 20 cm, 7.5 cm, and 7 cm in width, height, and thickness, respectively. It was used as an electrochemical reactor. Ti/RuO_2-IrO_2 (4 cm x 5 cm x 1 mm), graphite felt (4cm x 5cm x 3 mm), and foam nickel (4 cm x 5 cm x 1 mm) were used as anode, cathode, and insertion electrodes, respectively as shown in Figure 3.1. Characteristics of electrodes were shown in Tables 3.1 to 3.3 and Figures 3.2 to 3.4. The compartment of advanced electro-Fenton (AEF) reactor was shown in Figure 3.2. A magnetic bar was dropped on the bottom of the electrochemical reactor for stirred the mixture in the reactor.

a) Ti/RuO_2-IrO_2

b) Graphite felt

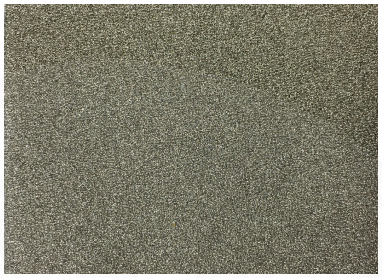

c) Foam nickel

Figure 3.1 Electrodes

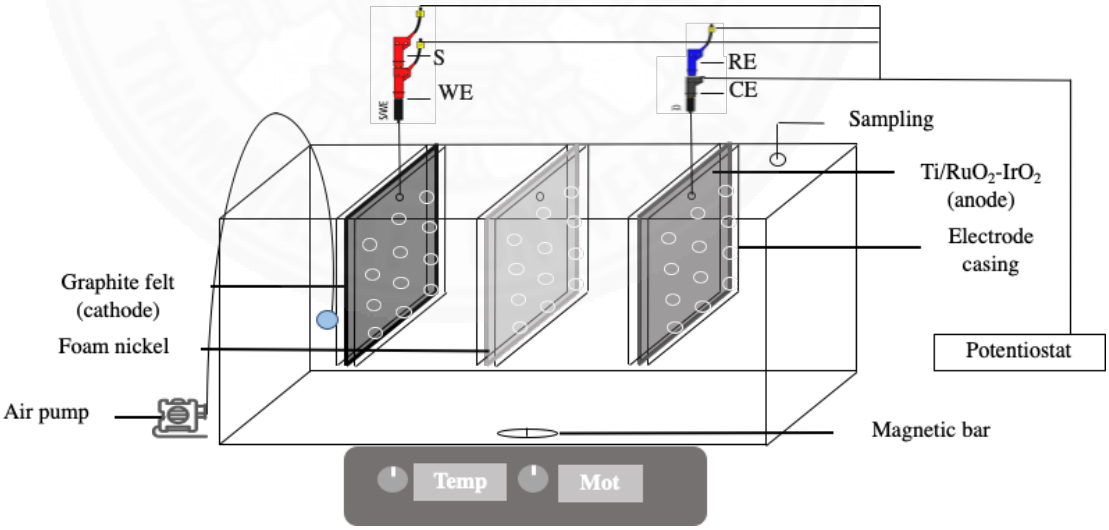

Figure 3.2 The compartment of advanced electro-Fenton (AEF) reactor (electrode was encased in PMMA sheets with holes opening as shown)

Table 3.1 Elemental compositions of Ti/RuO_2-IrO_2 electrode

Element	%Wt	%Atom
Ru	24.38	17.44
Ti	47.38	71.56
Ta	15.96	6.38
Ir	12.28	4.62

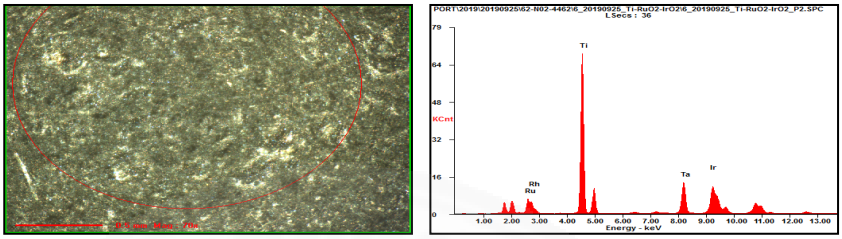

a) b)

Figure 3.3 Micro ED-XRF a) image and b) result of elemental compositions of Ti/RuO_2-IrO_2 electrode

Table 3.2 Elemental compositions of graphite felt electrode

Element	%Wt	%Atom
Si	6.96	4.54
P	34.64	20.48
K	3.90	1.79
C	46.21	70.47
Fe	8.29	2.72

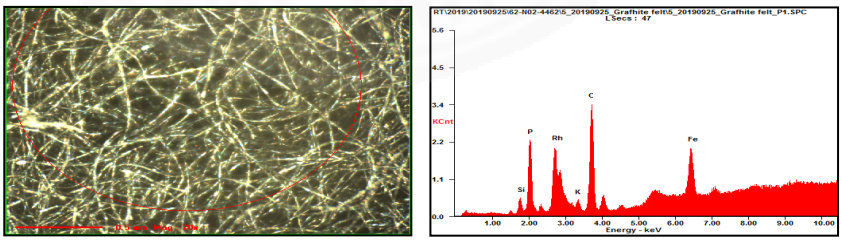

a) b)

Figure 3.4 Micro ED-XRF a) image and b) result of elemental compositions of graphite felt electrode

Table 3.3 Elemental compositions of foam nickel electrode

Element	%Wt	%Atom
Ca	0.18	0.27
Fe	0.11	0.12
Ni	99.47	99.61

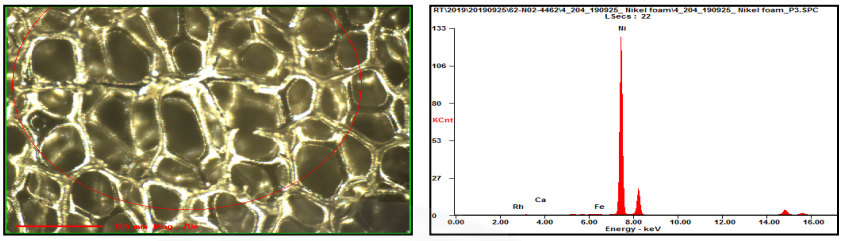

a) b)

Figure 3.5 Micro ED-XRF a) image and b) result of elemental compositions of foam nickel electrode

3.2 Experimental setup

3.2.1 Experimental procedure

The advanced electro-Fenton (AEF) process was conducted in a rectangular polymethyl methacrylate (PMMA or ACRYLIC) reactor with dimensions of 20 cm, 7.5 cm, and 7 cm in width, height, and thickness, respectively. The electrodes of Ti/RuO2-IrO2 (5 cm x 4 cm x 2 mm), graphite felt (5 cm x 4 cm x 3 mm), and foam nickel (5 cm x 4 cm x 1 mm) were used as anode, cathode, and insertion electrodes, respectively as shown in Figure 3.3. Wastewater used was obtained from the effluent from the biogas chamber from Millionaire Suphan Biogreen Power Co., Ltd (Suphanburi, Thailand). In each run, 560 mL of effluent from the biogas chamber at specified initial 14,250±250 ADMI and 5,067±230 mg/L of COD was prepared and fed to the reactor. 0.05 mol/L of Na_2SO_4 aqueous solution was used as the supporting electrolyte to increase the conductivity.

In this thesis, decolorization and COD reduction efficiencies of the effluent from the biogas chamber by the advanced electro-Fenton process were investigated to find the optimum condition by varying parameters as described in Table 3.4, such as initial pH

was adjusted by 1 mmol/L of H_2SO_4 or NaOH. $FeSO_4$.$7H_2O$ was added for the study of the initial concentration of ferrous ion. After wastewater was placed into the reactor, the applied voltage was adjusted by a power supply (potentiostat/instrument, Metrohm, PGSTAT 204). Air was purged at the rate of 1.5 L/min and a magnetic bar was dropped on the bottom of the electrochemical reactor for stirred the mixture in the reactor whole the reaction time under ambient temperature. Advanced electro-Fenton (AEF) reactor configuration is shown in Figure 3.5.

Table 3.4 Study parameters on decolorization and COD reduction efficiencies of effluent from the biogas chamber by advanced electro-Fenton (AEF) process

Controlled variables	**Results**
Initial color	14,250±250 ADMI
Initial chemical oxygen demand (COD)	5,067±230 mg/L
Initial volume of wastewater	560 mL
Independent variables	**Values**
Reaction time	0,15, 30, 45,30, 45, 60, 120, 180, 240, and 300 minutes
Initial pH	2, 3, 4, 5, 7, 9, and 11
Initial ferrous concentration	0.5, 1, 3, 5, 7, and 9 mM
Applied voltage	1.0, 2.0, 3.0, and 4.0 V
Dependent parameters	**Results**
	Color (ADMI)
	COD (mg/L)
	H_2O_2 concentration (mM)

The experimental setup in different processes (Table 3.5) were used to explore the efficiency of each process by using the optimum value received from Table 3.4.

Table 3.5 Various experimental conditions/types in this thesis. The advanced electro-Fenton (AEF) process employed foam nickel, while the traditional electro-Fenton (TEF) process does not use. The advanced electrochemical (AEM) process and advanced electro-Fenton process without applied voltage (AEF_0V) were also tested. (560 mL of effluent from the biogas chamber, initial 14,250±250 ADMI and 5,067±230 mg/L of COD)

Processes	Foam nickel	Initial pH of 3	3 mM of initial ferrous concentration	2.0V of applied voltage	120 minutes of reaction time
Advanced electro-Fenton (AEF)	/	/	/	/	/
Advanced electrochemical (AEM)	/	/	x	/	/
Traditional electro-Fenton (TEF)	x	/	/	/	/
Advanced electro-Fenton without applied voltage (AEF_0V)	/	/	/	x	/

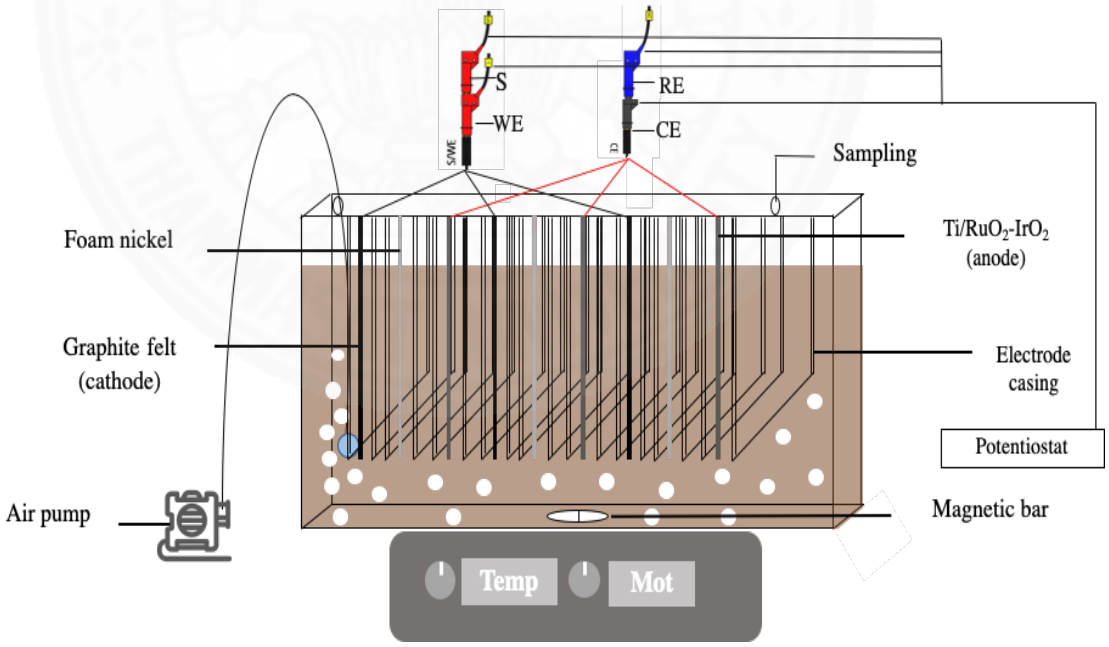

Figure 3.6 Advanced electro-Fenton (AEF) reactor configuration.

3.3 Experimental analysis

In this thesis, the water samples were analyzed by using several methods as shown in the Table 3.6.

Table 3.6 Analytical methods

Parameters	Methods
Color	UV-Vis spectrophotometer
COD	Dichromate Close Reflux
H_2O_2 concentration	Iodometric method
The concentration of ferrous ions (Fe^{2+})	Phenanthroline method
The elemental analysis	Micro ED-XRF

3.3.1 Measurement of color

The Pollution Control Department currently intends to revise this color standard to be more scientific and standardized. The color unit in ADMI (American Dye Manufacturers Institute) is proposed since it can be measured accurately and precisely without any sophisticated instrument. The standard value that allows to discharge is 300 ADMI (Ministry of Industry Thailand, 2019). For analyzing, the decolorization of sample was analyzed by UV-Vis spectrophotometer; Merck, Pharo 300. UV-Vis spectrophotometer is a tool used to measure the ADMI during UV rays and the visible light spectrum (400-700 nm) range that penetrates or is absorbed by a sample placed in the tool. The light wavelength is associated with the volume and type of substances in the sample, most of which are organic compounds, complex compounds and inorganic chemical that can absorb light in these wavelength ranges. First, used a 0.45 μm cellulose membrane for filtration. Then, the standard method for examination of water and wastewater for color measurement; APHA 2120F ADMI Weighted-Ordinate Spectrophotometer was used in this experiment (APHA, 1992).

3.3.2 Measurement of chemical oxygen demand (COD)

The standard method for examination of water and wastewater for color measurement; APHA 5220C Closed Reflux, Titrimetric Method. For analyzing the COD of sample was analyzed by titrimetric method. First, the sample was diluted by DI water

because this method is appropriate to the values in range of 40-400 mg/L. The sample and digestion solutions were added to digestion vessel (culture tube: 16x100 mm) by followed the APHA 5220C [42]., respectively. Placed tubes in the block heater, Spectroquant TR 420 thermoheater (150±2 °C). Then, following the APHA 5220C for measuring the concentration of COD.

3.3.3 Measurement of hydrogen peroxide (H_2O_2) concentration

Similar to Fe^{2+} analysis, the sample was analyzed for H_2O_2 immediately after sampling. The concentration of hydrogen peroxide residual was determined by titration with standard iodometric method in which the potassium iodide and sodium thiosulfate were use as the reactant and titrant, respectively, as described in APPENDIX A.

3.3.4 Measurement of ferrous ions (Fe^{2+})

Concentration of iron species, Fe^{2+}, soluble and total iron, were performed immediately after sampling without alkaline addition in order to prevent the precipitation of $Fe(OH)_2$. For ferrous analysis, the sample was analyzed by light absorbance measurement at 510 nm after being complexed with 1,10-phenanthroline and UV-vis spectrophotometer was used to analyze by following the standard method (APHA, 1992). The DI water, which mixed with the sample but excluded the o-phenanthroline, was being prepared for every sample. For total and soluble iron analysis, the samples were digested by concentrated hydrochloric acid (HCl) and hydroxylamine as the reductant to transform Fe^{3+} to Fe^{2+}. Then the samples were formed red-orange colored complexes with 1,10-phenanthroline following to the ferrous analysis.

3.3.5 Measurement of element

After preparing the sample with different methods depending on the form of sample. Micro ED-XRF (Energy Dispersive X-ray Fluorescence) was used for analyzing the types and elemental quantities in both liquid and solid samples. The wavelength dispersive can detect high concentrations of elements from the percentage to a small number as parts per million (ppm).

CHAPTER 4

RESULTS AND DISCUSSION

This study investigated the decolorization and COD removal of the effluent from the biogas digestion chamber from Millionaire Suphan Biogreen Power Co., Ltd (Suphanburi, Thailand) by advanced electro-Fenton (AEF) process. The initial characteristics of the effluent and chemical elements in the effluent from Millionaire Suphan Biogreen Power Co., Ltd (Suphanburi, Thailand) were analyzed by Environmental Research Institute, Chulalongkorn University and shown in Tables 4.1 and 4.2 and Figure 4.1.

In the experiment, the effluent was used as wastewater with the initial color and chemical oxygen demand (COD) values of 14,250±250 and 5,067±230 mg/L, respectively was fed to the reactor. Other characteristics of wastewater were analyzed and shown in Tables 4.3. The wastewater still had high color and concentration of organic/inorganic matter and was difficult to treat further by the biological wastewater treatment process.

The advanced electro-Fenton (AEF) process (EAOPs: Electrochemical Advanced Oxidation Processes) was used to treat the wastewater in this thesis. The optimum condition was optimized by the variables studied reaction time, included initial pH, initial ferrous concentration, and applied voltage, to achieve the highest efficiency. The decolorization and COD reduction efficiencies were calculated from Equations (4.1) and (4.2), respectively.

$$\text{Decolorization efficiency (\%)} = \left(1 - \frac{C}{C_0}\right) \times 100 \quad (4.1)$$

; where C is final ADMI and C_0 is initial ADMI.

$$\text{COD reduction efficiency (\%)} = \left(1 - \frac{C}{C_0}\right) \times 100 \quad (4.2)$$

; where C is final COD concentration and C_0 is initial COD concentration

Table 4.1 Initial characteristics of the wastewater from Millionaire Suphan Biogreen Power Co., Ltd (Suphanburi, Thailand)

Characteristics	Units	Values	Analyzed methods
Color	ADMI	207,500	ADMI Weighted-Ordinate Spectrophotometer Methhod 2120F.
pH	-	7.7	Electrometric Method 4500-H^+ B.
Conductivity	µs/cm	39,300	Laboratory Method 2510 B.
Turbidity	NTU	1,240	Nephelometric Method 2130 B.
TS (Total solid)	mg/L	71,340	Total Solids Dried at 103-105°C
COD	mg/L	64,521	Open Reflux Method 5220 B.
BOD_5	mg/L	4,703	5-Days BOD Test 5210 B.
Chloride	mg/L	9,550	Potentiometric Method 4500-Cl^- D.
Sulfate	mg/L	1,776	Turbidimetric Method 4500-SO_4^{2-} E.
Iron (Fe)	mg/L	35.71	Atomic Absorption Spectrometric Method 3500- Fe

Table 4.2 Chemical elements in the dry wastewater from Millionaire Suphan Biogreen Power Co., Ltd (Suphanburi, Thailand)

Element	%Wt	%Atom
P	2.02	1.46
Cl	0.12	0.07
S	1.81	1.26
C	29.92	55.77
K	61.41	34.46
N	4.19	6.70
Fe	0.69	0.27

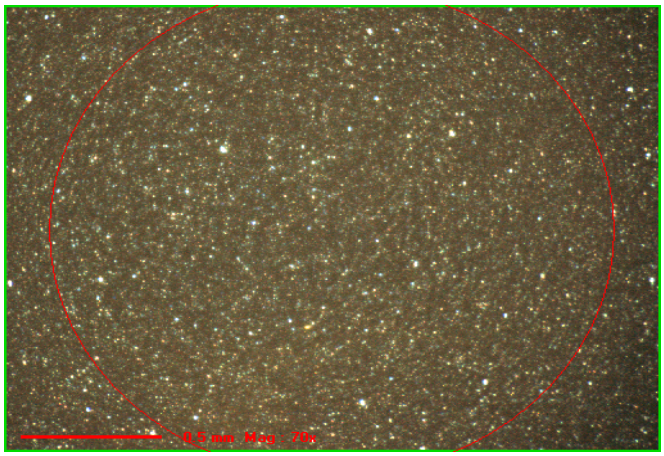

a)

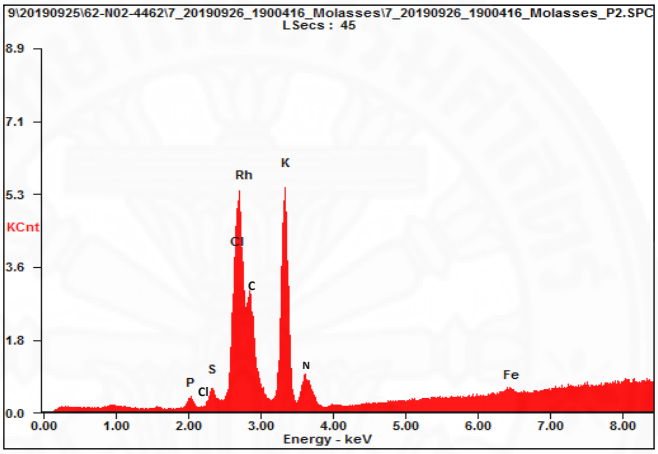

b)

Figure 4.1 Micro ED-XRF a) image and b) result of chemical elements in the wastewater from Millionaire SuphanBiogreen Power Co., Ltd (Suphanburi, Thailand)

Table 4.3 Characteristics of initial wastewater fed into the reactor

Characteristics	Unit	Results	Analyzed methods
Color	ADMI	14,250±250	UV-Vis spectrophotometer
COD	mg/L	5,067±230	Dichromate Close Reflux
pH	-	8	pH meter
The concentration of ferrous ions (Fe^{2+})	mg/L	86.92±0.99	Phenanthroline method

4.1. Efficiencies of decolorization and COD reduction in different processes

The objective of this experiment was to make sure that the color and organic pollutants contaminated in the effluent from the biogas chamber were degraded by the oxidation of hydroxyl radicals generated in the electro-Fenton processes with inserting foam nickel as the advanced electro-Fenton (AEF) process. To observe the oxidation of color and organic pollutants, the experiment results obtained from the advanced electro-Fenton process were compared with those obtained from other processes including advanced electrochemical (AEM) process, traditional electro-Fenton (TEF) process, and advanced electro-Fenton process without applied voltage (AEF_0V) (see Table 4.4 for comparison).

The experiments were conducted using 4 different processes. Each run was conducted using 3 sets of electrodes in the reactor. One set consisted of a Ti/RuO_2-IrO_2 as an anode electrode, a graphite felt as a cathode electrode, and a foam nickel as an inserting electrode. The distance between electrode was 0.5 cm. The initial volume of wastewater was 560 ml with the initial color unit (ADMI) and chemical oxygen demand (COD) were 14,250±250 ADMI and 5,067±230 mg/L, at ambient temperature. Other conditions were shown in Table 4.4. The initial pH, initial ferrous concentration, applied voltage, and reaction time are the same for all processes in this section, and will be varied in the next section focusing on advanced electro-Fenton (AEF) process.

Table 4.4 Conditions used for studying the efficiencies of decolorization and COD reduction efficiencies of the effluent from the biogas chamber in different processes

Processes	Electrodes			Initial pH of 3	3 mM of initial ferrous concent-ration	2.0V of applied voltage	120 minutes of reaction time
	Ti/RuO_2 -IrO_2	Graphite felt	Foam nickel				
Advanced electro-Fenton (AEF)	/	/	/	/	/	/	/
Advanced electrochemical (AEM)	/	/	/	/	x	/	/
Traditional electro-Fenton (TEF)	/	/	x	/	/	/	/
Advanced electro-Fenton without applied voltage (AEF_0V)	/	/	/	/	/	x	/

Figure 4.2 (a) shows that the efficiencies of decolorization using the 4 different processes, which are advanced electro-Fenton (AEF), advanced electrochemical (AEM), traditional electro-Fenton (TEF), and advanced electro-Fenton without applied voltage (AEF_0V), which obtained the color removal efficiency of 87.6±0.5%, 33.4±0.6%, 21.7±0.9%, and 10.9±2.1%, respectively. Figure 4.2 (b) depicts the COD removal efficiencies using advanced electro-Fenton (AEF), advanced electrochemical (AEM), traditional electro-Fenton (TEF), and advanced electro-Fenton without applied voltage (AEF_0V), which were 73.7±1.1%, 30.1±3.5%, 15.0±1.9%, and 10.7±5.8%, respectively.

It could be seen that the traditional electro-Fenton (TEF) and the advanced electrochemical (AEM) processes have lower removal efficiencies than the advanced electro-Fenton (AEF) process. It should also be noted that the advanced electro-Fenton process without applied voltage (AEF_0V) had the lowest efficiency, slightly lower than the traditional electro-Fenton (TEF) process. This is because without the applied voltage, there is very little hydrogen peroxide (H_2O_2) generated, and its efficiency is likely less than the traditional Fenton process, where the hydrogen peroxide (H_2O_2) was externally added into the reaction producing source of hydroxyl radicals efficiently.

In the advanced electro-Fenton (AEF) process, In the AEF process, the production of hydrogen peroxide (H_2O_2) and the hydroxyl radicals (•OH) may be generated by two pathways.

First, hydrogen peroxide (H_2O_2) was produced from the reduction of the dissolved oxygen on the cathode surface by a transfer pathway of two electrons as shown in Equation (4.1). The added ferrous (Fe^{2+}) then react with hydrogen peroxide (H_2O_2) to produce hydroxyl radicals (•OH) as shown in Equation (4.2).

$$O_2 + 2H^+ + 2e^- \rightarrow H_2O_2 \quad (4.1)$$

$$Fe^{2+} + H_2O_2 \rightarrow Fe^{3+} + {}^{\bullet}OH + OH^- \quad (4.2)$$

Another pathway to produce hydroxyl radicals ($^{\bullet}OH$) was through the Haber-Weiss reaction as shown in Equations (4.3)-(4.5). The Haber-Weiss reaction (Equation (4.5) generates superoxide anion ($\bullet O_2^-$) from the dissolved oxygen which is adsorbed on the surface of foam nickel, and hydrogen peroxide (H_2O_2) from the superoxide anion ($\bullet O_2^-$) react with one electron transfer pathway according to Equations (4.3) and (4.4).

$$Ni + 2O_2 \rightarrow Ni^{2+} + 2\bullet O_2^- \quad (4.3)$$

$$\bullet O_2^- + \bullet O_2^- + 2H^+ \rightarrow H_2O_2 + O_2 \quad (4.4)$$

$$\bullet O_2^- + H_2O_2 + 2H^+ \rightarrow O_2 + {}^{\bullet}OH + OH^- \quad (4.5)$$

Thus, the inserting of foam nickel in traditional electro-Fenton (TEF) process could help to produce hydrogen peroxide (H_2O_2) needed for the Fenton reaction. This process is thus called advanced electro-Fenton (AEF) process. The H_2O_2 in Equation (4.5) may come either from Equation (4.4) or from molecular oxygen reduction at cathode.

The increased hydrogen peroxide of AEF is highest when compared to other processes, as shown in Figure 4.2 (c) which in turn create hydroxyl radicals ($^{\bullet}OH$) to improve wastewater treatment efficiency, according to the above information of the production hydroxyl radicals ($^{\bullet}OH$).

By comparing the result with other processes, the AEF has increased color removal efficiency by 54.2±0.5%, 65.9±0.7%%, and 76.7±1.8% when compared with AEM, TEF, and AEF_0V, respectively. Additionally, AEF showed COD removal higher than AEM, TEF, and AEF_0V for 43.6±2.3%, 58.7±1.5%, and 63±3.5%, respectively.

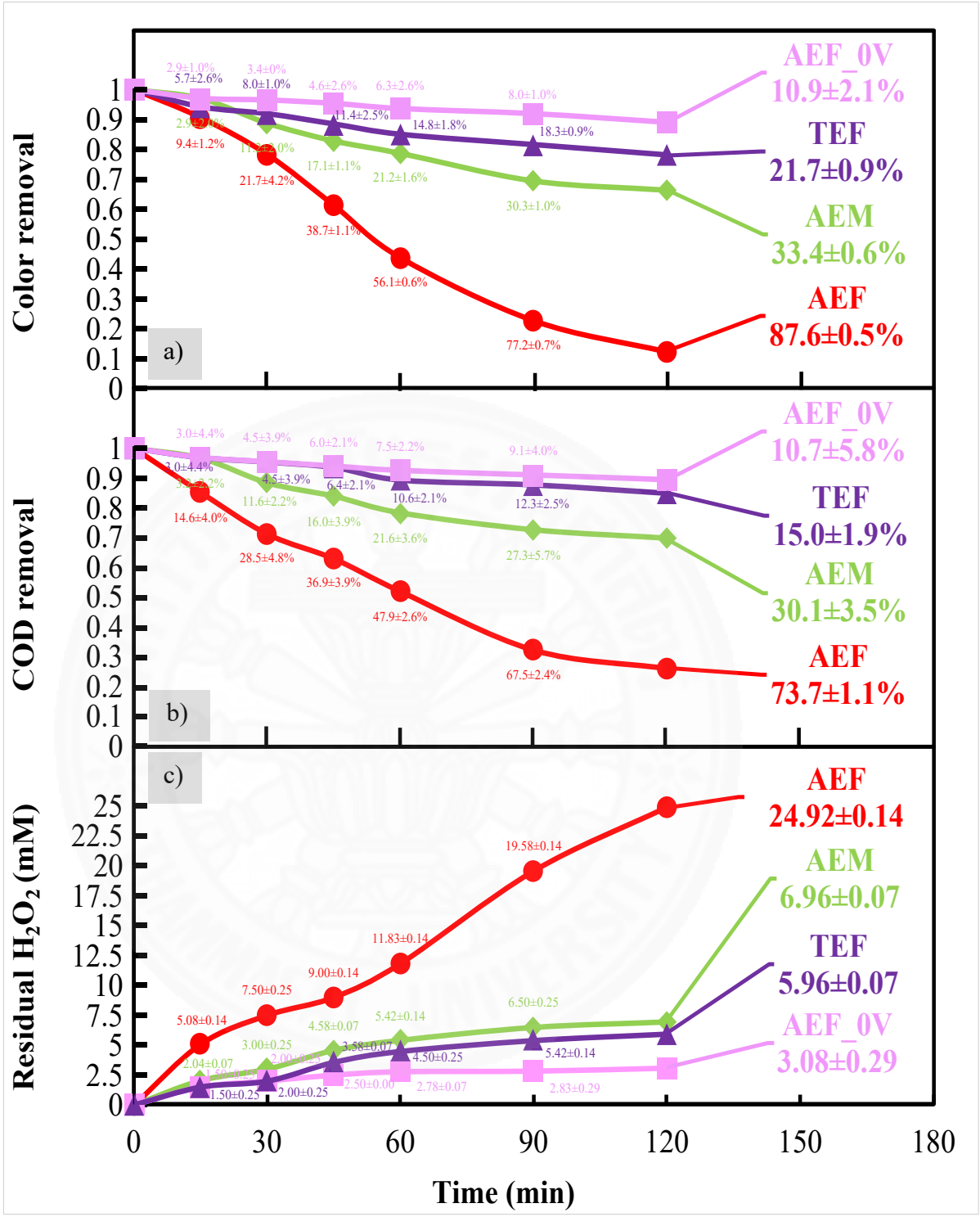

Figure 4.2 Effects of different processes on a) decolorization efficiency and b) COD reduction efficiency, and c) residual hydrogen peroxide (H_2O_2) produced in the system of the effluent from biogas chamber; using initial ferrous 3 mM, initial pH 3, applied voltage 2.0V, and reaction time 120 minutes at ambient temperature

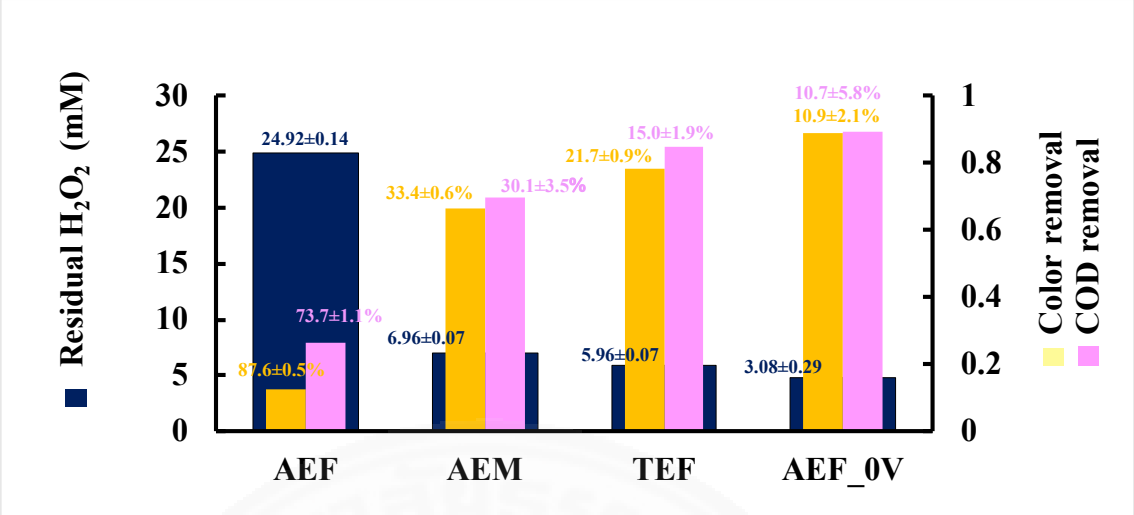

Figure 4.3 Efficiencies of different processes at 120 minutes of reaction time on decolorization efficiency and COD reduction efficiency, and residual hydrogen peroxide (H_2O_2) produced in the system of the effluent from biogas chamber; using initial ferrous 3 mM, initial pH 3, applied voltage 2.0V, and at ambient temperature

4.2 Studies of variables affecting the efficiency of AEF process

4.2.1 Effect of reaction time

Reaction time is an essential parameter for AEF process. The reaction time required for this process depends on many parameters; hydrogen peroxide concentration, ferrous concentration, pH, applied voltage, and wastewater strength. Therefore, to achieve the highest efficiencies of decolorization and COD reduction of effluent from biogas chamber, the reaction time required was investigated by varying the reaction time until the reaction reached equilibrium.

This section was conducted by varying reaction time and conducted under conditions as shown in Table 4.5. And the conditions as described in section 4.1 were also used to control the experiment.

To observe the effect of reaction time on the AEF process. Tthe sample was withdrawn from the batch reactor and the decolorization and COD reduction efficiency were analyzed following Table 4.5.

Table 4.5 Conditions used for studying the effect of reaction time on the efficiencies of decolorization and COD reduction of the effluent from the biogas chamber by AEF process

Controlled variables	**Results**
Initial color	14,250±250 ADMI
Initial chemical oxygen demand (COD)	5,067±230 mg/L
Initial volume of wastewater	560 mL
Initial pH	3
Initial ferrous concentration	3 mM
Applied voltage	2.0V
Independent variables	**Values**
Reaction time	0,15, 30, 45,30, 45, 60, 120, 180, 240, and 300 minutes
Dependent parameters	**Results**
	Color (ADMI)
	COD (mg/L)
	H_2O_2 concentration (mM)
	pH
	Ferrous concentration

The production of hydroxyl radicals, produced by both of hydrogen peroxide (H_2O_2) and ferrous ions (Fe^{2+}) play role as the crucial reagents for removing color and organics/inorganics pollutants in the wastewater. In this study, the concentrations of hydrogen peroxide produced during degradation in the AEF process was measured. It was found that the residual concentration of hydrogen peroxide (H_2O_2) increased when the reaction time increased. This was because H_2O_2 was produced greater than its consumption. Hydrogen peroxide (H_2O_2) was produced from the reduction of the dissolved oxygen on the cathode surface by a transfer pathway of two electrons as shown in Equation (4.6) and from the superoxide anion ($\bullet O_2^-$) which was produced from the dissolved oxygen which was adsorbed on the surface of foam nickel react with one electron transfer pathway according to Equation (4.7).

$$O_2 + 2H^+ + 2e^- \rightarrow H_2O_2 \quad (4.6)$$

$$\bullet O_2^- + \bullet O_2^- + 2H^+ \rightarrow H_2O_2 + O_2 \quad (4.7)$$

As a result, the efficiencies of decolorization and COD removal increased with the reaction time. After approximately 120 minutes of reaction time, the accumulated H_2O_2 nearly reached a steady-state. This indicates a balance between the consumption

and production of hydrogen peroxide. At the steady-state, H_2O_2 was electrogenerated and simultaneously consumed in the system at the same rate as shown in Figure 4.4 (c). Figures 4.4 (a) and (b) show that the efficiencies of decolorization and COD reduction dramatically increased as reaction time increased and attended constant after 2 hours of degradation time. Consequently, the recalcitrant organic/inorganic pollutants remained in the wastewater which could not further degrade.

The oxidation process depends on both concentration of hydrogen peroxide (H_2O_2) and ferrous ions (Fe^{2+}). Increasing the concentration of H_2O_2 is an effective factor for improving the process and removal efficiencies. Increasing the concentration of hydrogen peroxide enhances the oxidation potential of the process increases, which increases the removal of color and COD. On the other hand, by increasing its concentration, the percentage of removal efficiencies increases until the reaction reaches equilibrium conditions as shown in Figure 4.5. The decolorization and COD reduction efficiencies were improved by increasing the reaction time. The removal efficiencies and hydrogen peroxide slightly increased after 120 minutes. The indicated slightly increased of H_2O_2 could be also considered to the following reasons: As the reaction time increases, the H_2O_2 is self-decomposed according to Equation (4.8). It is also hypothesized that hydrogen peroxide may be decomposed by the electrolysis within high applied voltage.

$$H_2O_2 + H_2O_2 \rightarrow 2O_2 + 4H^+ + 4e^- \quad (4.8)$$

Furthermore, hydrogen peroxide (H_2O_2) reacts with hydroxyl radicals ($^{\bullet}OH$) and acts as scavenger for the hydroxyl radicals ($^{\bullet}OH$) to produce hydroperoxyl radicals ($HO_2^{\bullet}$), Equation (4.9).

$$H_2O_2 + {}^{\bullet}OH \rightarrow HO_2^{\bullet} + H_2O; \quad (4.9)$$

Additionally, the ferrous was added in the process as initial ferrous concentration and residual ferrous concentration was increased by extending the reaction time. The increased residual ferrous was generated by regeneration of ferrous ions (Fe^{2+}) which was produced by the reaction of ferric ions (Fe^{3+}) and H_2O_2, as shown in Equation (4.10). Conversely, Figure 4.6 also shows that the concentration of Fe^{2+} and H_2O_2 dramatically increased at the beginning but slightly increased after 120 minutes as reached constant

because of the lack of Fe^{3+} after H_2O_2 was continuously generated in the system, then it reacted with Fe^{3+} to produce Fe^{2+}. Fe^{2+} was produced by the plentiful amount of H_2O_2 until reached maximum (steady-state) and H_2O_2 was used to react with Fe^{3+} also reached steady-state, that making Fe^{2+} unable to be converted to $Fe^{3+}$by the reaction of Fe^{2+} and H_2O_2 is inhibited, as described in Equation (4.11).

$$Fe^{3+} + H_2O_2 \rightarrow Fe^{2+} + HO_2^{\bullet} \quad (4.10)$$

$$Fe^{2+} + H_2O_2 \rightarrow Fe^{3+} + {}^{\bullet}OH + OH^- \quad (4.11)$$

The product from Equations (4.9) and (4.10), hydroperoxyl radicals ($HO_2^{\bullet}$), were able to continuously react in the system as shown in Equations (4.12) and (4.13)

$$HO_2^{\bullet} \leftrightarrow {}^{\bullet}O_2^- + H^+ \quad (4.12)$$

$$HO_2^{\bullet} + HO_2^{\bullet} \rightarrow H_2O_2 + O_2 \quad (4.13)$$

From Equation (4.12), superoxide anion (${}^{\bullet}O_2^-$) can also react as shown in Equation (4.14). H_2O_2 from Equations (4.13) and (4.14) can generate H^+ as shown in Equation (4.15).

$${}^{\bullet}O_2^- + {}^{\bullet}O_2^- + 2H^+ \rightarrow H_2O_2 + O_2 \quad (4.14)$$

$$H_2O_2 \leftrightarrow HO_2^- + H^+ \quad (4.15)$$

At the same time, it is noted that the suitable pH for this process is 3. However, during the reaction, the acidic of wastewater was increased (about 3 to 2) by Equations (4.12) and (4.15), as shown in Figure 4.6, which was not suitable for converting H_2O_2 to active hydroxyl radicals (${}^{\bullet}OH$) as the hydrogen peroxide can react with H^+ and generating oxonium ion ($H_3O_2^+$), as shown in Equation (4.16) which inhibits the reaction of H_2O_2 and Fe^{2+} affecting less hydroxyl radicals (${}^{\bullet}OH$) produced.

$$H^+ + H_2O_2 \rightarrow H_3O_2^+ \quad (4.16)$$

In this case, pH could be adjusted using from 2 to 3 to become suitable condition, the sodium hydroxide (NaOH) can be added in the process to maintain the optimum pH3. However, too much alkaline solution (NaOH) will cause a ferrous ion to transform to be a floc of ferric oxyhydroxide ($FeHO_2$) and ferric hydroxide ($Fe(OH)_3$) which will then precipitate. Thereby, there contributes less free iron ions and will be lost. As a consequence, the $^{\bullet}OH$ and its oxidation potential will also drop according to increasing pH.

According to the decolorization and COD reduction efficiencies directly depend on the concentration of hydroxyl radicals ($^{\bullet}OH$) generated by the concentration of hydrogen peroxide (H_2O_2) and ferrous (Fe^{2+}), as Equation (4.11).

Moreover, the appropriate reaction time is also one of the effective factors in the implementation of the process. The results of decolorization and COD removal were not significantly different after 120 minutes. Hence, the reaction time of 120 minutes was recommended as optimum reaction time.

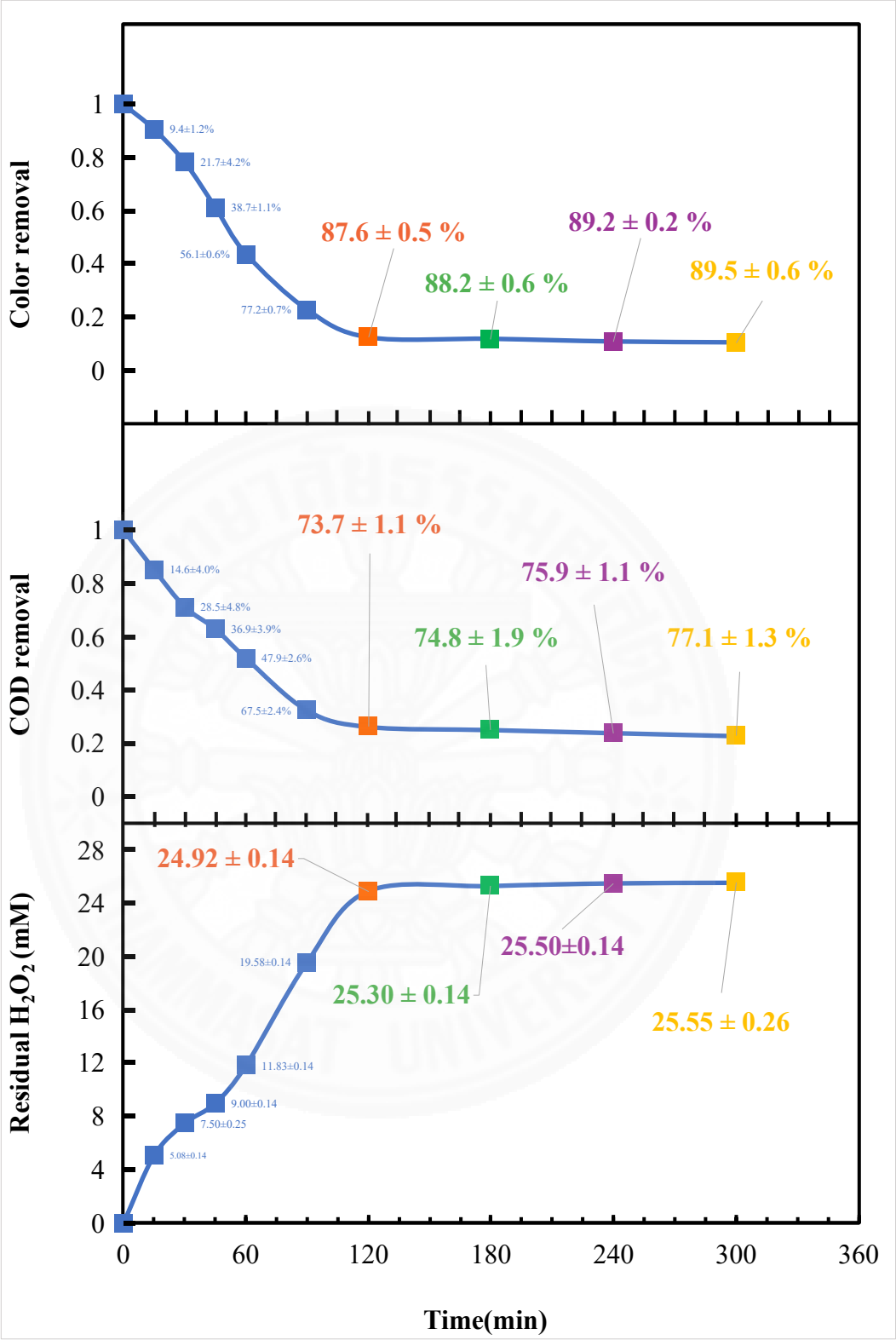

Figure 4.4 Effect of reaction time on a) decolorization efficiency and b) COD reduction efficiency, and c) residual hydrogen peroxide (H_2O_2) produced in the system of the effluent from biogas chamber by AEF process; using initial ferrous 3 mM, initial pH 3, applied voltage 2.0V, and at ambient temperature

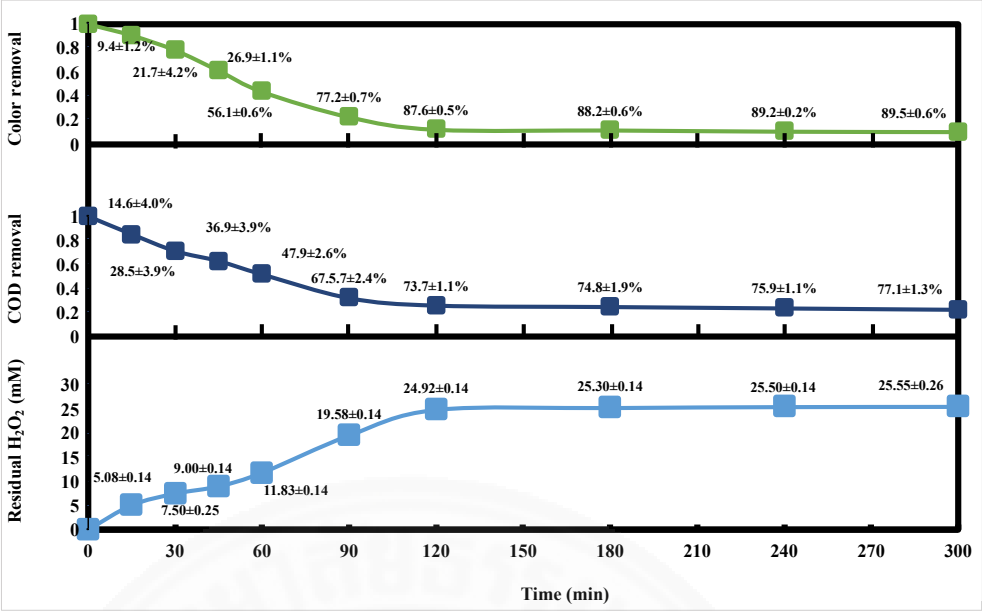

Figure 4.5 Efficiencies of reaction time on decolorization efficiency and COD reduction efficiency, and residual hydrogen peroxide (H_2O_2) produced in the system of the effluent from biogas chamber by AEF process; using initial ferrous 3 mM, initial pH 3, applied voltage 2.0V, and at ambient temperature

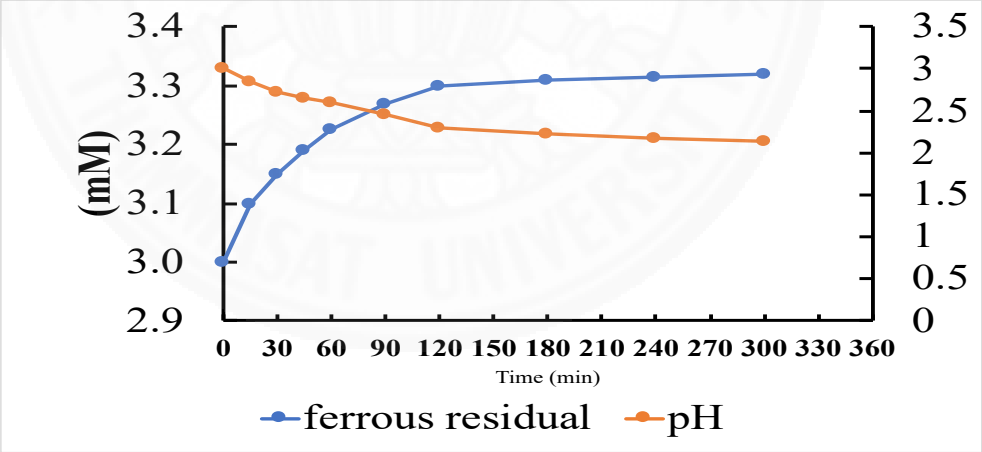

Figure 4.6 The residual ferrous and pH on removal efficiency of effluent from biogas chamber by AEF process under the conditions of 560 ml of wastewater (initial 14,250±250 ADMI and 5,067±230 mg/L of COD), 3 mM of initial ferrous concentration, initial pH is 3, 3 sets of electrodes, distance between electrode is 0.5 cm, applied voltage 2.0V, and at ambient temperature in 300 minutes

4.2.2 Effect of initial pH

Evaluation of initial pH variation was investigated to examine the optimum pH for the decolorization and COD (chemical oxygen demand) reduction efficiencies of the effluent from the biogas chamber by the advanced electro-Fenton (AEF) process. The initial pH was varied from 2 to 11 to study the effect of each initial pH range due to its role in controlling the catalytic activity.

The experiments were conducted using 3 sets of electrodes as described in section 4.1. The distance between electrodes was 0.5 cm and they were conducted at ambient temperature. The addition of $FeSO_4.7H_2O$ was added to the study of the concentration of ferrous ions acting as a catalyst. The conditions used in the experiment were described in Table 4.6.

Table 4.6 Conditions used for studying the effect of initial pH on the efficiencies of decolorization and COD reduction of the effluent from the biogas chamber by AEF process

Controlled variables	**Results**
Initial color	14,250±250 ADMI
Initial chemical oxygen demand (COD)	5,067±230 mg/L
Initial volume of wastewater	560 mL
Initial ferrous concentration	3 mM
Applied voltage	2.0V
Reaction time	120 minutes
Independent variables	**Values**
Initial pH	2, 3, 4, 5, 7, 9, and 11
Dependent parameters	**Results**
	Color (ADMI)
	COD (mg/L)
	H_2O_2 concentration (mM)

Hydroxyl radicals can be generated by hydrogen peroxide. Figure 4.7 (c) illustrates that hydroxyl radicals were generated most at pH of 3.

From the results of the experiment, it can be seen that the decolorization and COD removal efficiencies were increased when increasing pH 2 to 3 and also decreased when increasing pH 3 to 11 as shown in Figures 4.7 (a) and (b). According to Figures 4.7 (a) and (b), the trends for initial pH of 2, 4, 5, and 7 were similar. The efficiencies of decolorization and COD removal decreased steadily until the decolorization efficiency reached the range between 72.9±0.7% to 53.4±0.4% and COD removal efficiency reached

63.8±2.3% to 50.6±2.0%. Meanwhile, the removal efficiency at initial pH 3 was 5 times higher than initial pH 11. Moreover, at initial pH 3, the removal efficiency increased rapidly for 15%, comparing to initial pH 2.

The AEF process is susceptible to pH. Hydroxyl radicals ($^{\bullet}OH$) produced by Equation (4.17) is highly generated at acidic pH (lower than 3), while at pH higher than 3, the generation of $^{\bullet}OH$ is lower because Fe^{2+} is more transformed to Fe^{3+} which precipitates as ferric hydroxide ($Fe(OH)_3$) occurs as shown in Equation (4.18). ($Fe(OH)_3$) stimulates the decomposition of H_2O_2 to water and oxygen to deactivation of catalyst leading to decreasing in the production of $^{\bullet}OH$. Therefore, $^{\bullet}OH$ decreased when oxidize organic compounds decreased causing the efficiencies of decolorization and COD reduction to decrease.

Although, the decolorization and COD removal efficiencies were increased when increasing of acidic condition. On the other hand, in case of pH less than 3; (by comparing initial pH 2 with initial pH 3), the efficiencies of decolorization and COD removal decreased. In this case, H_2O_2 can transform into $H_3O_2^+$ by capturing one proton (H^+), as shown in Equation (4.19). This causes the production of H_2O_2 to decrease. Meanwhile, H_2O_2 inhibited by $H_3O_2^+$ will reduce the regeneration of Fe^{2+} by the reaction of Fe^{3+} with H_2O_2, as Equation (4.20). Therefore, $^{\bullet}OH$ is also decreased by the reduction of H_2O_2 and Fe^{2+}.

Hence, it could be concluded that the initial pH 3 was the optimum value for decolorization and COD removal.

$$Fe^{2+} + H_2O_2 \rightarrow Fe^{3+} + {}^{\bullet}OH + OH^- \quad (4.17)$$

$$Fe^{3+} + 3OH^- \rightarrow Fe(OH)_{3(s)} \quad (4.18)$$

$$H^+ + H_2O_2 \rightarrow H_3O_2^+ \quad (4.19)$$

$$Fe^{3+} + H_2O_2 \rightarrow Fe^{2+} + HO_2^{\bullet} \quad (4.20)$$

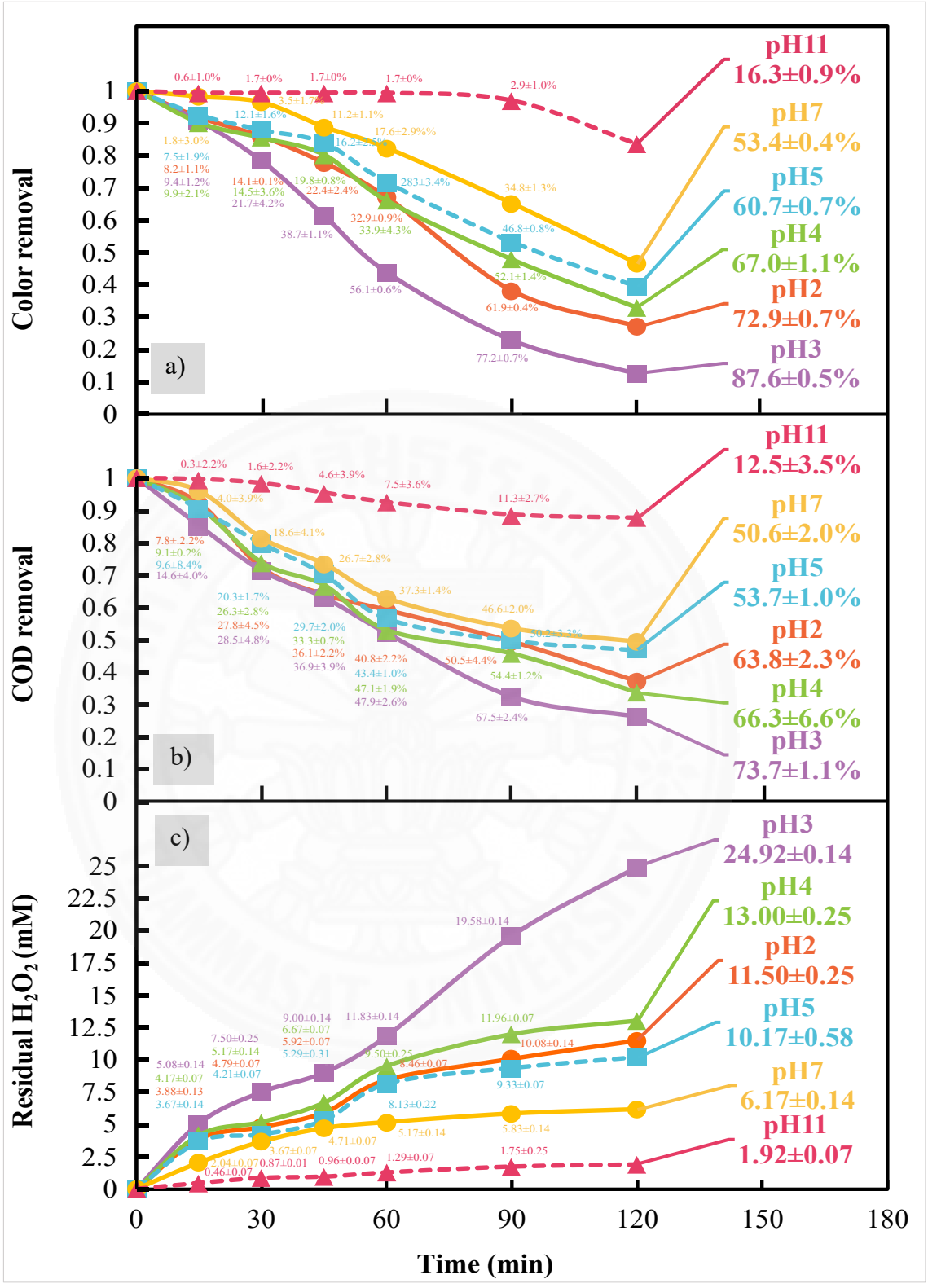

Figure 4.7 Effect of initial pH on a) decolorization efficiency and b) COD reduction efficiency, and c) residual hydrogen peroxide (H_2O_2) produced in the system of the effluent from biogas chamber by AEF process; using initial ferrous 3 mM, applied voltage 2.0V, and reaction time 120 minutes at ambient temperature

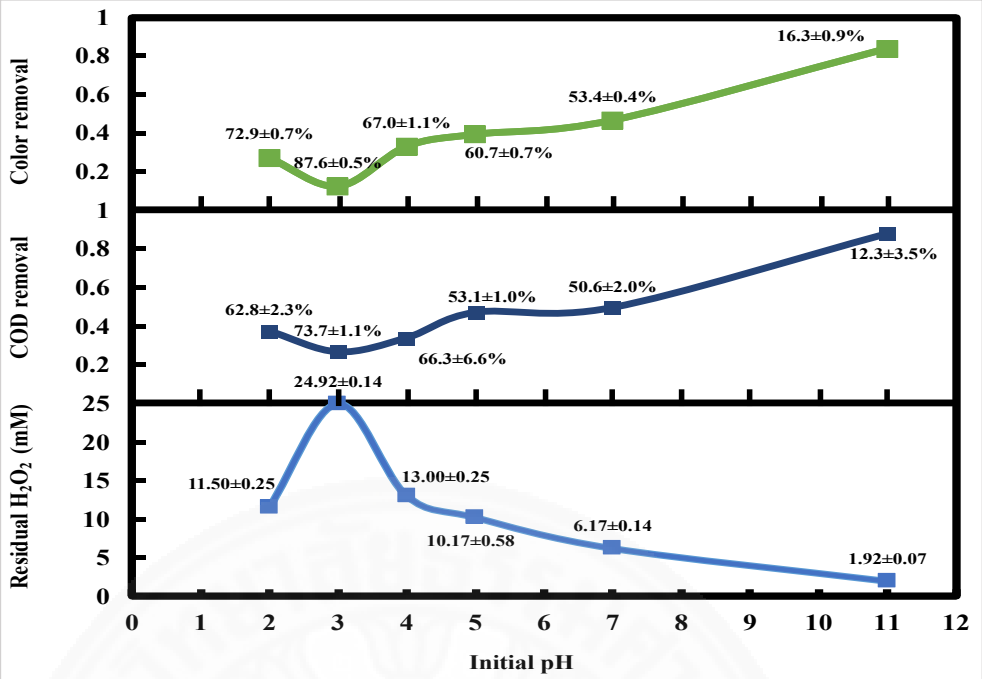

Figure 4.8 Efficiencies of initial pH at 120 minutes of reaction time on decolorization efficiency and COD reduction efficiency, and residual hydrogen peroxide (H_2O_2) produced in the system of the effluent from biogas chamber by AEF process; using initial ferrous 3 mM, applied voltage 2.0V, and at ambient temperature

4.2.3 Effect of initial ferrous concentration

In this section, the initial ferrous concentration was varied to determine its effect on the decolorization and COD (chemical oxygen demand) reduction efficiencies of the effluent from biogas chamber by AEF process. Effect of initial ferrous concentration was investigated because hydrogen peroxide is not a very strong oxidant. The oxidizing power of hydrogen peroxide was not enough to destroy the pollutants in this wastewater. Therefore, ferrous ions are an essential catalyst that affects the chemical reactions in the wastewater. The chemical reactions are the combination of H_2O_2 and Fe^{2+} to generate strong radicals $^{\bullet}OH$, which have very high oxidizing capacity to degrade the pollutants. Hence, initial concentration of ferrous ions was expected to affect the performance of the process significantly.

This section was conducted by varying the initial concentration of ferrous (Fe^{2+}) between 0.5 to 9 mM and also conducted under conditions of 3 sets of electrodes as descried in section 4.1. The experimental conditions were shown in Table 4.7.

Table 4.7 Conditions used for studying the effect of initial ferrous ions concentration on the efficiencies of decolorization and COD reduction of the effluent from the biogas chamber by AEF process

Controlled variables	**Results**
Initial color	14,250±250 ADMI
Initial chemical oxygen demand (COD)	5,067±230 mg/L
Initial volume of wastewater	560 mL
Initial pH	3
Applied voltage	2.0V
Reaction time	120 minutes
Independent variables	**Values**
Initial ferrous concentration	0.5, 1, 3, 5, 7, and 9 mM
Dependent parameters	**Results**
	Color (ADMI)
	COD (mg/L)
	H_2O_2 concentration (mM)

The results found that both color and COD removal efficiencies increased with the increase initial ferrous concentration from 0.5 mM to 3 mM, the efficiencies of decolorization and COD reduction increased as 41.1±1.7% to 87.6±0.5% for color and 34.0±4.2% to 73.7±1.1% for COD, respectively. However, when the initial ferrous concentration enhanced from 3 mM to 9 mM, the efficiencies of decolorization and COD reduction significantly decreased as 87.6±0.5% to 48.2±0.8% for color and 73.7±1.1% to 47.6±2.1% for COD, respectively as shown in Figure 4.9 (a) and (b). This is due to the fact that excess amount of ferrous concentration can be oxidized by hydroxyl radicals resulting in a yellow precipitate of Fe^{3+} ($Fe(OH)_3$) as shown in Equations (4.21) and (4.22). Iron sludge increases with reaction time and during electrolysis, this precipitate gets deposited at the bottom of the reactor and on the electrode surface.

Once it has been deposited, this Fe^{3+} cannot be regenerated to Fe^{2+}, as shown in Equation (4.23). Hence, the availability of Fe^{2+} is less to react with available H_2O_2. This is the reason behind the reduced efficiency observed with an incremental change in ferrous ion concentration. Therefore, the optimum initial concentration of ferrous in this work should be 3 mM.

Moreover, it was also found that hydroxyl radicals (•OH) were generated by the concentration of hydrogen peroxide. The highest amount of hydroxyl radicals generated was found at the initial concentration of ferrous of 3 mM, as shown in Figure 4.9 (c).

$$Fe^{2+} + {}^{\bullet}OH \rightarrow Fe^{3+} + OH^{-} \quad (4.21)$$

$$Fe^{3+} + 3OH^{-} \rightarrow Fe(OH)_{3(s)} \quad (4.22)$$

$$Fe^{3+} + H_2O_2 \rightarrow Fe^{2+} + HO_2^{\bullet} \quad (4.23)$$

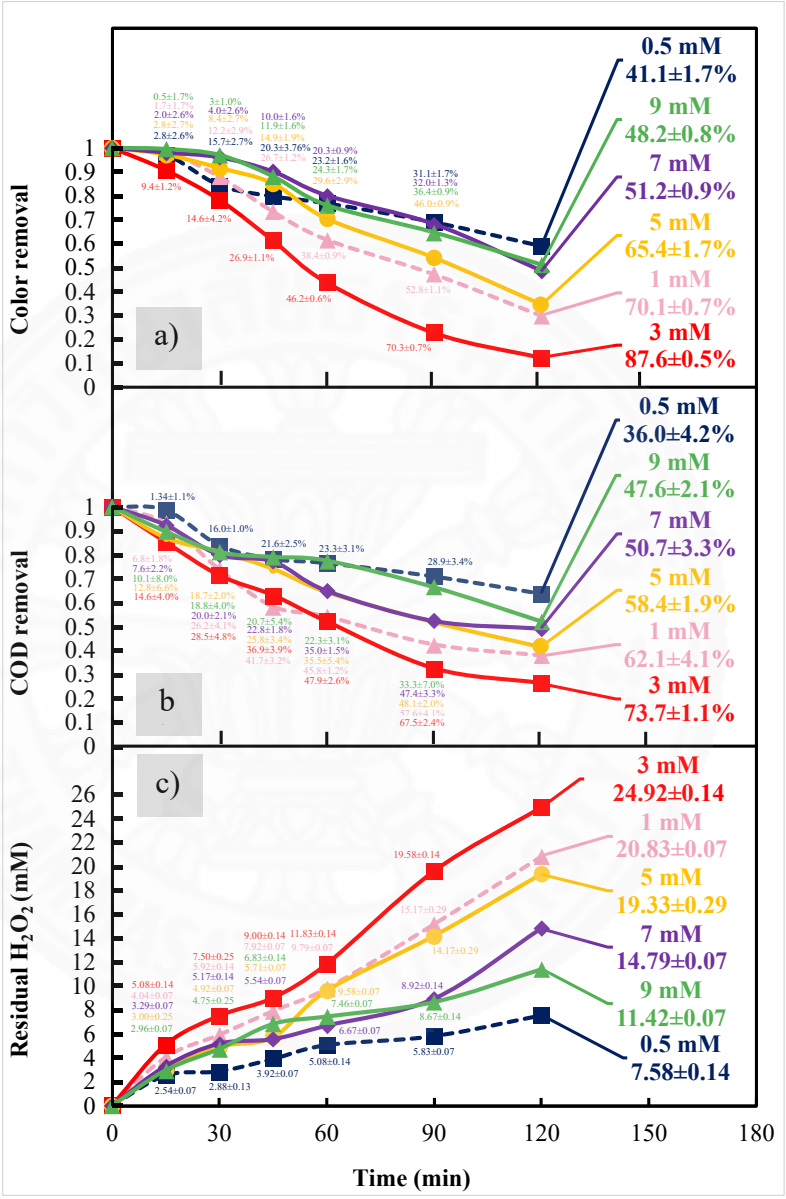

Figure 4.9 Effect of initial ferrous concentrations on a) decolorization efficiency and b) COD reduction efficiency, and c) residual hydrogen peroxide (H_2O_2) produced in the system of the effluent from biogas chamber by AEF process; using initial pH 3, applied voltage 2.0V, and reaction time 120 minutes at ambient temperature

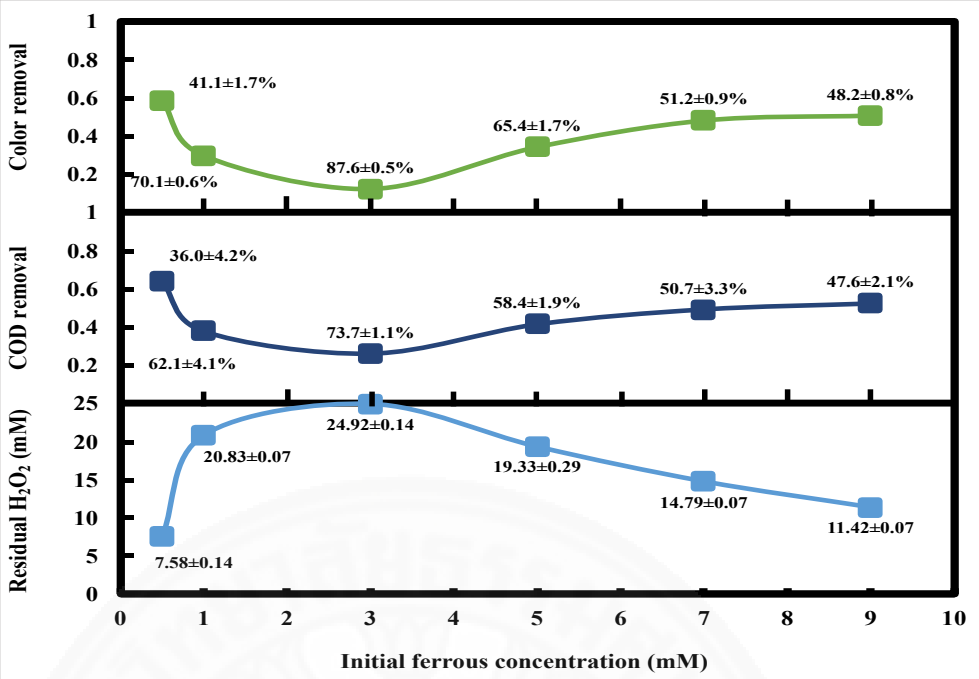

Figure 4.10 Efficiencies of initial ferrous concentrations at 120 minutes of reaction time on decolorization efficiency and COD reduction efficiency, and residual hydrogen peroxide (H_2O_2) produced in the system of the effluent from biogas chamber by AEF process; using initial pH 3, applied voltage 2.0V, and at ambient temperature

4.2.4 Effect of applied voltage

The intensity of applied voltage is a significant factor controlling the performance of AEF process. Increasing the applied voltage increases the production rate of hydrogen peroxide on the cathode and the regeneration of ferrous to produce hydroxyl radicals.

This experimental part tries to investigate the effect of intensity of applied voltage on the AEF process. The studied conditions were under varying the applied voltage between 1.0 to 4.0 V and also conducted under conditions as described in section 4.1. The experimental conditions were listed in Table 4.8.

Table 4.8 Conditions used for studying the effect of applied voltage on the efficiencies of decolorization and COD reduction of the effluent from the biogas chamber by AEF process

Controlled variables	**Results**
Initial color	14,250±250 ADMI
Initial chemical oxygen demand (COD)	5,067±230 mg/L
Initial volume of wastewater	560 mL
Initial pH	3
Initial ferrous concentration	3 mM
Reaction time	120 minutes
Independent variables	**Values**
Applied voltage	1.0, 2.0, 3.0, and 4.0 V
Dependent parameters	**Results**
	Color (ADMI)
	COD (mg/L)
	H_2O_2 concentration (mM)

From the result, the removal efficiencies both in terms of decolorization and COD reduction followed by 1.0, 2.0, 3.0, and 4.0V found that the 2.0V provided the highest removal efficiencies. The trends of removal efficiencies for applied voltage of 1.0, 2.0, 3.0, and 4.0V are similar as it increases gradually in each applied voltage.

The increase of the applied voltage from 1.0 to 2.0 V could enhance the efficiencies of decolorization and COD reduction up to 23% and 17%, respectively by comparing to the other applied voltage and the production of the electrogenerated H_2O_2; as shown in Figure 4.11 (c), this is because higher applied voltage causes the dissociation of hydrogen peroxide to generate more concentration of hydroxyl radicals in the solution according to the Equation (4.24), which are highly reactive and responsible for the degradation of refractory pollutants. Moreover, higher regeneration of ferrous ion from ferric ion with the higher voltage increases the efficiency of reactions.

$$O_2 + 2H^+ + 2e^- \rightarrow H_2O_2 \quad (4.24)$$

Although the high applied voltage would increase the efficiency of the Fenton chain reaction, Figures 4.11 (a) and (b) illustrate that the efficiencies of decolorization and COD reduction decreased when the applied voltage increased from 2.0 to 4.0V. This is probably due to the discharge of oxygen at the anode, Equation (4.25) and the hydrogen evolution at cathode, Equation (4.26), inhibit the main reaction of this process. Moreover,

the higher potential not only leads to more decomposition of H_2O_2 but also causes higher energy consumption. Therefore, the applied voltage of 2.0V was selected in this work.

$$2H_2O \rightarrow O_2 + 4H^+ + 4e^- \quad (4.25)$$

$$2H^+ + 2e^- \rightarrow H_2 \quad (4.26)$$

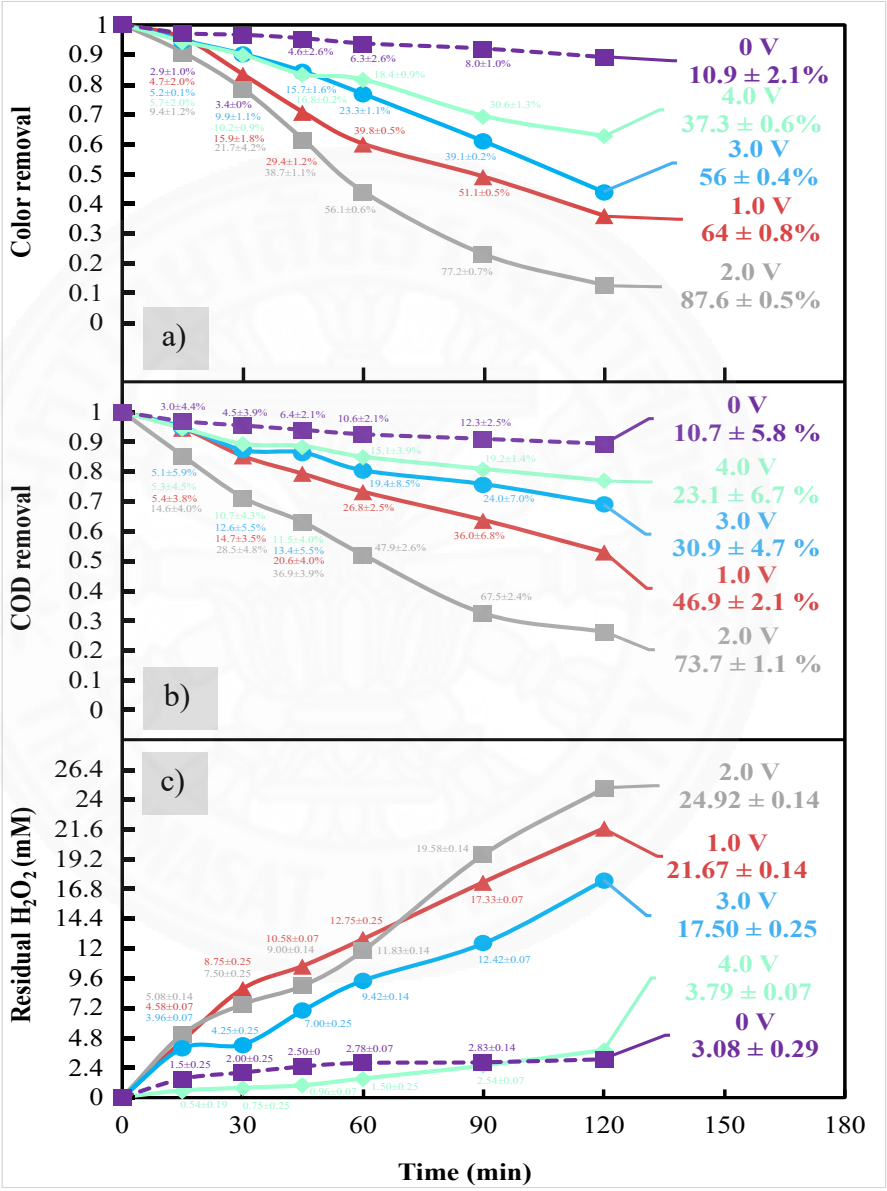

Figure 4.11 Effect of applied voltage on a) decolorization efficiency and b) COD reduction efficiency, and c) residual hydrogen peroxide (H_2O_2) produced in the system of the effluent from biogas chamber by AEF process; using initial ferrous 3 mM, initial pH 3, and reaction time 120 minutes at ambient temperature

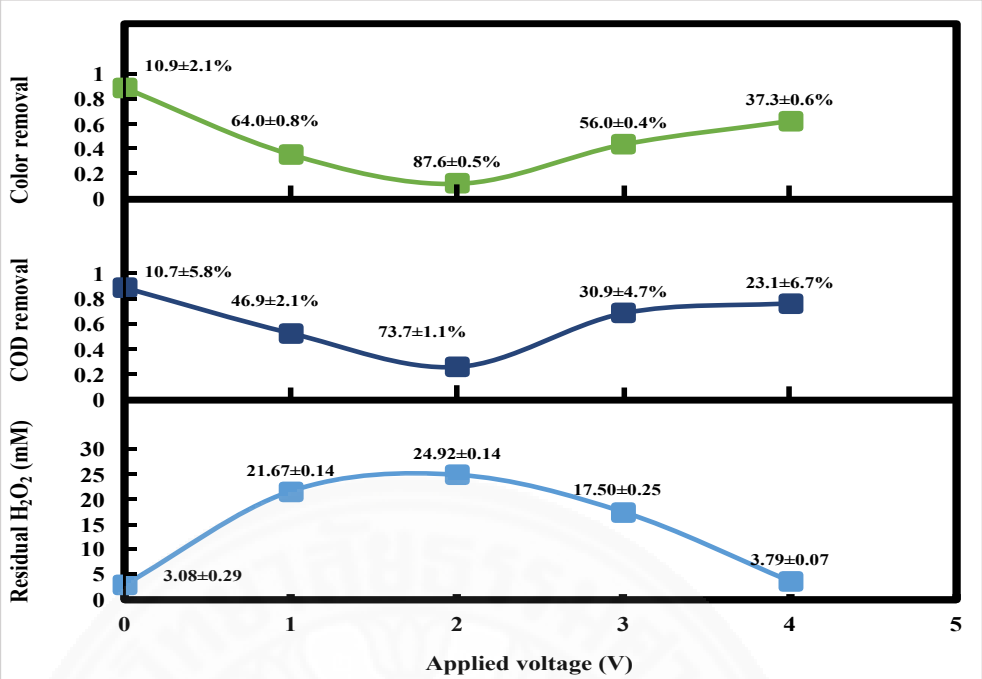

Figure 4.12 Efficiencies of applied voltage at 120 minutes of reaction time on decolorization efficiency and COD reduction efficiency, and residual hydrogen peroxide (H_2O_2) produced in the system of the effluent from biogas chamber by AEF process; using initial ferrous 3 mM, initial pH 3, and at ambient temperature

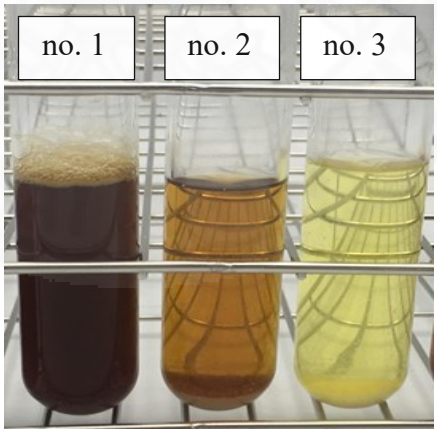

Figure 4.13 Comparison between initial wastewater (ADMI=14,250±250 ADMI, COD=5,067±230 mg/L), (no. 1) and the optimum condition of TEF process (no.2), and as well as AEF (no.3)

CHAPTER 5

CONCLUSIONS

Advanced electro-Fenton (AEF) process consisting of three electrodes, which are cathode made of graphite felt, anode made of Ti/RuO_2-IrO_2, and insertion electrode made of foam nickel was employed to treat wastewater effluent. Need to conclude what is the function of foam nickel here, and briefly the AEF process. AEF process is an effective process for decolorization and COD reduction of the effluent from biogas chamber by using hydroxyl radicals ($^{\bullet}OH$) to decompose the pollutants. The Ti/RuO_2-IrO_2 has been successful used as anode to degrade pollutants in industrial wastewater which had dark color owing to its stability and excellent transmission of electrons. The hydrogen peroxide (H_2O_2) was produced from the reduction of the dissolved oxygen adsorbed on the cathode (graphite felt) surface, and also from foam nickel was inserted as the insertion electrode, H_2O_2 was produced from superoxide anion ($\bullet O_2^-$) from dissolved oxygen adsorbed on the foam nickel surface and the one electron reduction of molecular oxygen at the cathode react with one electron pathway. The hydrogen peroxide (H_2O_2) then reacts with additional of ferrous (Fe^{2+}) as Fenton reaction, and also with superoxide anion ($\bullet O_2^-$) as Haber-Weiss reaction to generate hydroxyl radicals ($^{\bullet}OH$).

The wastewater was used in this work was from commercial biogas chamber and had a very dark color with the initial color and chemical oxygen demand (COD) values of 14,250±250 and 5,067±230 mg/L, respectively from a commercial biogas chamber. Several parameters such as initial pH, initial ferrous concentration, applied voltage, and reaction time were shown to have a significant impact on the performance of AEF process both in term of decolorization and COD reduction.

The optimum condition was found to be the initial pH of 3, the initial ferrous concentration of 3 mM, the applied voltage of 2.0V and 120 minutes of reaction time by electro-Fenton process which could achieve the highest color removal efficiency of 87.6±0.5% (from 14,250±250 to 1,767±58 ADMI), and the COD removal efficiency of 73.7±1.1% (from 5,067±230 mg/L to 1,335±112 mg/L).

Comparing to other processes tested which were: advanced electrochemical (AEM) process (by adding foam nickel in the electrochemical process), traditional electro-Fenton (TEF) process, and advanced electro-Fenton process without applied voltage (AEF_0V), the AEF process showed the highest color removal, as shown in the

results of AEF process has increased color removal efficiency by 54.2±0.5%, 65.9±0.7%%, and 76.7±1.8% when compared with AEM, TEF, and AEF_0V processes, respectively. Additionally, AEF process has improved COD removal by 43.6±2.3%, 58.7±1.5%, and 63±3.5% when compared with AEM, TEF, and AEF_0V processes, respectively.

AEF process showed higher color and COD removal efficiencies than other processes tested. This corresponds to the fact that the AEF process uses three-dimensional electrochemical oxidation system (inserting foam nickel electrode between two-dimensional electrodes) which can enhance the production of hydroxyl radicals (•OH). The production of hydroxyl radicals (•OH) of advanced electro-Fenton process are higher than other processes which produced more superoxide anion ($\bullet O_2^-$) than TEF process and AEF_0V process.

AEF can generate superoxide anion ($\bullet O_2^-$) from two pathways, first, from the dissolved oxygen which is adsorbed on the surface of foam nickel and second, the one electron reduction of molecular oxygen at the cathode , while TEF process can produce only one pathway; the one-electron reduction of molecular oxygen and AEF_0V can also produce only one pathway; the dissolved oxygen which is adsorbed on the surface of foam nickel.

The production of hydroxyl radicals (•OH) of AEF process also higher than AEM process, because the production of hydroxyl radicals (•OH) of AEM process can be generated only by one pathway; Haber-Weiss reaction.

The higher production of hydroxyl radicals (•OH) have highly potential to oxidize the organic pollutants in wastewater, and shorten mass transfer distance than other processes. As shown in the results of AEF process has increased residual hydrogen peroxide (H_2O_2) by 24.92±0.14, 6.96±0.07, 5.96±0.07, and 4.83±0.29 mM when compared with AEM, TEF, and AEF_0V processes, respectively. The increased hydrogen peroxide (H_2O_2) produced also more hydroxyl radicals (•OH) to improve wastewater treatment efficiency.

It can be concluded that the advanced electro-Fenton process is an effective process for decolorization and COD reduction of the effluent from biogas chamber with are a new and interesting process.

REFERENCES

APHA (1992), Standard Methods for the Examination of Water and Wastewater, 23nd Edition, American Public Health Association, American Water Works Association, Water Environment Federation, Washington D.C.

Adina Elena Segneanu, C. O., Carmen Lazau, Paula Sfirloaga, Paulina Vlazan, Cornelia Bandas and Ioan Grozescu. (2013). Waste Water Treatment Methods. In W. E. a. R. K. Chowdhury (Ed.), *Water Treatment*.

Arimi, M., Zhang, Y., Götz, G., & Geissen, S.-U. (2015). Treatment of melanoidin wastewater by anaerobic digestion and coagulation. *Environmental technology, 36*, 1-31.

Barrera-DÌaz, C., CaÒizares, P., Fern·ndez, F., Natividad, R., Rodrigo, M., & Toluca-Atlacomulco, C. (2017). Electrochemical Advanced Oxidation Processes: An Overview of the Current Applications to Actual Industrial Effluents. *Revista de la Sociedad QuÌmica de Mexico, 58*, 256-275.

Bautista, P., Mohedano, A., Gilarranz, M., Casas, J., & Rodriguez, J. J. (2007). Application of Fenton Oxidation to Cosmetic Wastewaters Treatment. *Journal of Hazardous Materials, 143*, 128-134.

Bekedam, E. K. COFFEE BREW MELANOIDINS

Bekedam, E. K. (2008). Coffee brew melanoidins Structural and Functional Properties of Brown-Colored Coffee Compounds.

Bergmann, J. C., Trichez, D., Sallet, L. P., de Paula e Silva, F. C., & Almeida, J. R. M. (2018). Chapter 4 - Technological Advancements in 1G Ethanol Production and Recovery of By-Products Based on the Biorefinery Concept. In A. K. Chandel & M. H. Luciano Silveira (Eds.), *Advances in Sugarcane Biorefinery* (pp. 73-95): Elsevier.

Buxton, G., Greenstock, C. L., Helman, W., & Ross, A. B. (1988). Critical Review of rate constants for reactions of hydrated electrons, hydrogen atoms and hydroxyl radicals J≈OH/≈q in Aqueous Solution. *Journal of Physical and Chemical Reference Data, 17*, 513-886.

Cämmerer, B., Jalyschko, W., & Kroh, L. (2002). Intact Carbohydrate Structures as Part of the Melanoidin Skeleton. *Journal of Agricultural and Food Chemistry, 50*, 2083-2087.

Can, W., Yao-Kun, H., Qing, Z., & Min, J. (2014). Treatment of secondary effluent using a three-dimensional electrode system: COD removal, biotoxicity assessment, and disinfection effects. Chemical Engineering Journal, 243, 1-6.

Cardona, C., Machuca-Martínez, F., & Marriaga-Cabrales, N. (2013). Treatment of vinasse by using electro-dissolution and chemical flocculation. *15*, 191-200.

Chen, G., Hoag, G. E., Chedda, P., Nadim, F., Woody, B. A., & Dobbs, G. M. (2001). The mechanism and applicability of in situ oxidation of trichloroethylene with Fenton's reagent. *Journal of Hazardous Materials, 87*(1), 171-186.

Coca, M., Teresa, G., x, a, M., González, G., Peña, M., . . . a, J. A. (2004). Study of coloured components formed in sugar beet processing. *Food Chemistry, 86*(3), 421-433.

Davarnejad, R., & Azizi, J. (2016). Alcoholic wastewater treatment using electro-Fenton technique modified by Fe2O3 nanoparticles. *Journal of Environmental Chemical Engineering, 4*(2), 2342-2349.

Davarnejad, R., Mohammadi, M., & Ismail, A. F. (2014). Petrochemical wastewater treatment by electro-Fenton process using aluminum and iron electrodes: Statistical comparison. *Journal of Water Process Engineering, 3*, 18-25.

Echavarría Vélez, A. P., Pagán, J., & Ibarz, A. (2013). Antioxidant activity of the melanoidin fractions formed from DGlucose and D-Fructose with L-Asparagine in the Maillard reaction. *Scientia agropecuaria, 4*, 45-54.

España-Gamboa, E., Vicent, T., Font Segura, X., Maldonado, J., Canto-Canché, B., & Alzate-Gaviria, L. (2017). Pretreatment of vinasse from the sugar refinery industry under non-sterile conditions by Trametes versicolor in a fluidized bed bioreactor and its effect when coupled to an UASB reactor. *Journal of Biological Engineering, 11*.

Gawande, S. (2015). *An overview of the Fenton Process for Industrial Wastewater*.

Gawande, S. (2016). Advancement in Fenton Process (AOPs) for Wastewater- A review. *International Journal of Engineering and Technical Research (IJETR), 5*, 59-61.

Glaze, W., Kang, J.-W., & Chapin, D. (1987). The Chemistry of Water Treatment Processes Involving Ozone, Hydrogen Peroxide and Ultraviolet Radiation. *Ozone-science & Engineering - OZONE-SCI ENG, 9*, 335-352.

Hoigne, J. (1998). *Chemistry of Aqueous Ozone and Transformation of Pollutants by Ozonation and Advanced Oxidation Processes*.

Huang, C. P., Dong, C., & Tang, Z. (1993). Advanced chemical oxidation: Its present role and potential future in hazardous waste treatment. *Waste Management, 13*(5), 361-377.

Janke, L., Leite, A., Nikolausz, M., Schmidt, T., Liebetrau, J., Nelles, M., & Stinner, W. (2015). Biogas Production from Sugarcane Waste: Assessment on Kinetic Challenges for Process Designing. *International Journal of Molecular Sciences, 16*, 20685-20703.

Kamei, H., Koide, T., Hashimoto, Y., Kojima, T., Umeda, T., & Hasegawa, M. (1998). Tumor Cell Growth-Inhibiting Effect of Melanoidins Extracted from Miso and Soy Sauce. *Cancer biotherapy & radiopharmaceuticals, 12*, 405-409.

Kong, W., Wang, B., Ma, H., & Gu, L. (2006). Electrochemical treatment of anionic surfactants in synthetic wastewater with three-dimensional electrodes. *Journal of Hazardous Materials, 137*(3), 1532-1537.

Kothandapani, S., & Preetha, B. (2015). Effect of initial pH on biohydrogen production using distillery wastewater by batch process. *Journal of Chemical and Pharmaceutical Sciences, 8*, 148-151.

Kourdali, S., Badis, A., & Boucherit, A. (2014). Degradation of direct yellow 9 by electro-Fenton: Process study and optimization and, monitoring of treated water toxicity using catalase. *Ecotoxicology and Environmental Safety, 110*, 110-120.

Langner, E., & Rzeski, W. (2013). Biological Properties of Melanoidins: A Review. *International Journal of Food Properties, 17*, 344-353.

Lipczynska-Kochany, E. (1991). Degradation of aqueous nitrophenols and nitrobenzene by means of the Fenton reaction. *Chemosphere, 22*(5), 529-536.

Liu, W., Ai, Z., & Zhang, L. (2012). Design of a neutral three-dimensional electro-Fenton system with foam nickel as particle electrodes for wastewater treatment. *Journal of Hazardous Materials, 243*, 257-264.

Liu, Z., Wang, F., Li, Y., Xu, T., & Zhu, S. (2011). Continuous electrochemical oxidation of methyl orange waste water using a three-dimensional electrode reactor. *Journal of Environmental Sciences, 23*, S70-S73.

Lunar, L., Sicilia, D., Rubio, S., Pérez-Bendito, D., & Nickel, U. (2000). Degradation of photographic developers by Fenton's reagent: Condition optimization and kinetics for metol oxidation. *Water Research, 34*, 1791-1802.

Masten, S. J., & Davies, S. H. R. (1994). THE USE OF OZONATION TO DEGRADE ORGANIC CONTAMINANTS IN WASTEWATERS. *Environmental Science & Technology, 28*(4), 180A-185A.

Metcalf & Eddy., Tchobanoglous, G., Burton, F. L. 1., & Stensel, H. D. (2003). Wastewater engineering: Treatment and reuse (4th ed.). Boston: McGraw-Hill.

Ministry of Industry Thailand, The declaration of Standard of control wastewater discharge from industry, 2019 B.C.

Mishra, N., Reddy, R., Kuila, A., Rani, A., Mukherjee, P., & Nawaz, A. (2017). A Review on Advanced Oxidation Processes for Effective Water Treatment. *Current World Environment, 12*, 470-490.

Munter, R. (2001). Advanced oxidation processes-current status and prospects. *Proc. Estonian Acad. Sci. Chem., 50*, 59-80.

Naspolini, B., Machado, A., Junior, W., Freire, D., & Cammarota, M. (2017). Bioconversion of Sugarcane Vinasse into High-Added Value Products and Energy. *BioMed Research International, 2017*, 1-11.

Nishikimi, M., Appaji, N., & Yagi, K. (1972). The occurrence of superoxide anion in the reaction of reduced phenazine methosulfate and molecular oxygen. *Biochem Biophys Res Commun, 46*(2), 849-854.

Olennikov, D., & Tankhaeva, L. (2012). Physicochemical characteristics and antioxidant activity of melanoidin pigment from the fermented leaves of Orthosiphon stamineus. *Revista Brasileira de Farmacognosia, 22*, 284-290.

Oturan, M., Peiroten, J., Chartrin, P., & Acher, A. (2000). Complete Destruction of p-Nitrophenol in Aqueous Medium by Electro-Fenton Method. *Environmental Science & Technology - ENVIRON SCI TECHNOL, 34*.

Oturan, M. A., Oturan, N., Lahitte, C., & Trevin, S. (2001). Production of hydroxyl radicals by electrochemically assisted Fenton's reagent: Application to the mineralization of an organic micropollutant, pentachlorophenol. *Journal of Electroanalytical Chemistry, 507*(1), 96-102.

Oturan, M. A., & Pinson, J. (1995). Hydroxylation by Electrochemically Generated OH.bul. Radicals. Mono- and Polyhydroxylation of Benzoic Acid: Products and Isomer Distribution. *The Journal of Physical Chemistry, 99*(38), 13948-13954.

Parsaee, M., Kiani Deh Kiani, M., & Karimi, K. (2019). A review of biogas production from sugarcane vinasse. *Biomass and Bioenergy, 122*, 117-125.

Peres, J., Beltrán, J., & Domínguez, J. (2004). Integrated Fenton's Reagent – Coagulation/Flocculation Process for the Treatment of Cork Processing Wastewaters. *Journal of Hazardous Materials, 107*, 115-121.

Pignatello, J. J. (1992). Dark and photoassisted iron(3+)-catalyzed degradation of chlorophenoxy herbicides by hydrogen peroxide. *Environmental Science & Technology, 26*(5), 944-951.

Pirvu, C., Brillas, E., Radovici, O., & Banu, A. (2004). Degradation of 4-chlorophenol by advanced electrochemical oxidation methods. *Revista de Chimie -Bucharest- Original Edition-, 55*, 764-768.

Reis, C., Bento, H., Alves, T., Carvalho, A., & Castro, H. (2019). Vinasse Treatment within the Sugarcane-Ethanol Industry Using Ozone Combined with Anaerobic and Aerobic Microbial Processes. *Environments, 6*, 5.

Rizzi, G. P. (1997). Chemical structure of colored maillard reaction products. *Food Reviews International, 13*(1), 1-28.

Rufián Henares, J., & Morales, F. (2007). Antimicrobial activity of melanoidins. *Journal of Food Quality, 30*, 160-168.

Rufián-Henares, J. A., & Morales, F. J. (2007). Functional properties of melanoidins: In vitro antioxidant, antimicrobial and antihypertensive activities. *Food Research International, 40*(8), 995-1002.

Rurián-Henares, J. A., & Morales, F. J. (2008). Antimicrobial Activity of Melanoidins against Escherichia coli Is Mediated by a Membrane-Damage Mechanism. *Journal of Agricultural and Food Chemistry, 56*(7), 2357-2362.

Santal, A. R., & Singh, N. (2013). *Biodegradation of Melanoidin from Distillery Effluent: Role of Microbes and Their Potential Enzymes*.

Santal, A. R., & Singh, N. P. (2013). Biodegradation of Melanoidin from Distillery Effluent: Role of Microbes and Their Potential Enzymes. In *Biodegradation of Hazardous and Special Products*.

Silván, J. M., van de Lagemaat, J., Olano, A., & del Castillo, M. D. (2006). Analysis and biological properties of amino acid derivates formed by Maillard reaction in foods. *Journal of Pharmaceutical and Biomedical Analysis, 41*(5), 1543-1551.

Smaniotto, A., Bertazzo, A., Comai, S., & Traldi, P. (2009). The role of peptides and proteins in melanoidin formation. *Journal of mass spectrometry : JMS, 44*, 410-418.

Stasinakis, A. (2008). Use of Selected Advanced Oxidation Processes (AOPs) for Wastewater Treatment – a Mini Review. *Global NEST Journal Copyright©, 10*, 376-385.

Susree, M., Asaithambi, P., Saravanathamizhan, R., & Matheswaran, M. (2013). Studies on various mode of electrochemical reactor operation for the treatment of distillery effluent. *Journal of Environmental Chemical Engineering, 1*(3), 552-558.

Wang, H.-Y., Qian, H., & Yao, W.-R. (2011). Melanoidins produced by the Maillard reaction: Structure and biological activity. *Food Chemistry, 128*(3), 573-584.

Xiong, Y., He, C., Karlsson, H. T., & Zhu, X. (2003). Performance of three-phase three-dimensional electrode reactor for the reduction of COD in simulated wastewater-containing phenol. *Chemosphere, 50*(1), 131-136.

Xiong, Y., Strunk, P. J., Xia, H., Zhu, X., & Karlsson, H. T. (2001). Treatment of dye wastewater containing acid orange II using a cell with three-phase three-dimensional electrode. *Water Research, 35*(17), 4226-4230.

Zhang, H., Zhang, D., & Zhou, J. (2006). Removal of COD from landfill leachate by electro-Fenton method. *Journal of Hazardous Materials, 135*(1), 106-111.

Zhao, H.-Z., Sun, Y., Xu, L.-N., & Ni, J.-R. (2010). Removal of Acid Orange 7 in simulated wastewater using a three-dimensional electrode reactor: Removal mechanisms and dye degradation pathway. *Chemosphere, 78*(1), 46-51.

APPENDICES

APPENDIX A
HYDROGEN PEROXIDE CONCENTRATION ANALYSIS

A.1 Principle

Hydrogen peroxide oxidized iodine to iodide in the presence of acid and molybdate catalyst. The iodine formed is titrated with the thiosulfate solution incorporating a starch indicator as demonstrate in the following equation:

$$H_2O_2 + 2KI + H_2SO_4 \rightarrow I_2 + K_2SO_4 + 2H_2O \quad (A.1)$$

$$I_2 + 2Na_2S_2O_3 \rightarrow Na_2S_4O_6 + 2NaI \quad (A.2)$$

A.2 Interference

Other oxidizing agents will also produce iodine, whereas reducing agent (and unsaturated organics) will react with the liberated iodine. The contribution from other oxidizing agent can be determined by omitting the acid and molybdate catalyst.

A.3 Reagent

1. Potassium iodide solution
2. Ammonium molybdate solution
3. Sulfuric acid solution
4. Starch indicator
5. Sodium thiosulfate solution

A.4 Procedure

1. Add 50 ml of DI water to Erlenmeyer flask. Next, 10 ml of sulfuric acid solution and 15 ml of potassium iodide were added. Then 3 drops of ammonium molybdate were added.
2. Add 1 ml of sample to Erlenmeyer flask.
3. Titrate with sodium thiosulfate solution to faint yellow or straw color. Stir gently during titration to minimize iodine loss.
4. Add 3 drops of starch indicator and continue titration until the blue color just disappears.
5. Repeat steps 1-4 to analyze hydrogen peroxide.

A.5 Calculation

$$H_2O_2, \left(\frac{mg}{L}\right) = \frac{(A - B)\text{ml. titrate of } Na_2S_2O_3 \times N \times 17 \times 1000}{\text{ml. sample}} \qquad (A.3)$$

Where:

A= ml of of $Na_2S_2O_3$ for sample

B= ml of of $Na_2S_2O_3$ for blank

N = Normality of $Na_2S_2O_3$

APPENDIX B
EXPERIMENTAL RAW DATA

B.1 Data of efficiencies of decolorization and COD removal in different processes

Table B.1.1 Raw data of residual hydrogen peroxide (H_2O_2)

Advanced electro-Fenton (ACF)		
Hydrogen peroxide residual		
Time (min)	mM	SD
0	0.00	
15	5.08	0.14
30	7.50	0.25
45	9.00	0.14
60	11.83	0.14
90	19.58	0.14
120	24.92	0.14

Advanced electrochemical (AEM)		
Hydrogen peroxide residual		
Time (min)	mM	SD
0	0.00	
15	2.04	0.07
30	3.00	0.25
45	4.58	0.07
60	5.42	0.14
90	6.50	0.25
120	6.96	0.07

Traditional electro-Fenton (TEF)		
Hydrogen peroxide residual		
Time (min)	mM	SD
0	0.00	
15	1.50	0.25
30	2.00	0.25
45	3.58	0.07
60	4.50	0.25
90	5.42	0.14
120	5.96	0.07

Advanced electro-Fenton without applied voltage (AEF_0V)		
Hydrogen peroxide residual		
Time (min)	mM	SD
0	0.00	
15	1.50	0.25
30	2.00	0.25
45	2.50	0.00
60	2.78	0.07
90	2.83	0.14
120	3.08	0.29

Table B.1.2 Raw data of decolorization efficiency

Advanced electro-Fenton (AEF)					
ADMI					
Time (min)	ADMI	SD	% removal	SD	C/C_0 (ADMI)
0	14250	250			1
15	12917	382	9.4	1.2	0.906
30	11157	382	21.7	4.2	0.783
45	8735	289	38.7	1.1	0.613
60	6243	58	56.1	0.6	0.438
90	3249	58	77.2	0.7	0.228
120	1767	58	87.6	0.5	0.124

Advanced electrochemical (AEM)					
ADMI					
Time (min)	ADMI	SD	% removal	SD	C/C_0 (ADMI)
0	14167	144			1
15	13750	250	2.9	2.0	0.971
30	12583	144	11.2	1.0	0.888
45	11750	250	17.1	1.1	0.829
60	11167	144	21.2	1.6	0.788
90	9867	58	30.3	1.0	0.696
120	9433	58	33.4	0.6	0.666

Traditional electro-Fenton (TEF)					
ADMI					
Time (min)	ADMI	SD	% removal	SD	C/C_0 (ADMI)
0	14583	144			1
15	13750	250	5.7	2.6	0.943
30	13417	144	8.0	1.0	0.920
45	12917	289	11.4	2.5	0.886
60	12417	144	14.8	1.8	0.851
90	11917	144	18.3	0.9	0.817
120	11417	144	21.7	0.9	0.783

Advanced electro-Fenton without applied voltage (AEF_0V)					
ADMI					
Time (min)	ADMI	SD	% removal	SD	C/C_0 (ADMI)
0	14583	144			1
15	14167	144	2.9	1.0	0.971
30	14083	144	3.4	0.0	0.966
45	13917	289	4.6	2.6	0.954
60	13667	289	6.3	2.6	0.937
90	13417	144	8.0	1.0	0.920
120	13000	433	10.9	2.1	0.891

Table B.1.3 Raw data of COD reduction efficiency

Advanced electro-Fenton (AEF)					
COD					
Time (min)	mg/L	SD	% removal	SD	C/C_0 (COD)
0	5067	231			1
15	4319	2	14.6	4.0	0.852
30	3613	112	28.5	4.8	0.713
45	3195	233	36.9	3.9	0.631
60	2640	2	47.9	2.6	0.521
90	1647	2	67.5	2.4	0.325
120	1335	117	73.7	1.1	0.264

Advanced electrochemical (AEM)					
COD					
Time (min)	mg/L	SD	% removal	SD	C/C_0 (COD)
0	5000	200			1
15	4834	119	3.2	2.2	0.967
30	4419	115	11.6	2.2	0.884
45	4193	2	16.0	3.9	0.839
60	3913	112	21.6	3.6	0.783
90	3629	1	27.3	5.7	0.726
120	3489	1	30.1	3.5	0.698

Traditional electro-Fenton (TEF)					
COD					
Time (min)	mg/L	SD	% removal	SD	C/C_0 (COD)
0	5067	115			1
15	4909	112	3.0	4.4	0.969
30	4835	119	4.5	3.9	0.954
45	4743	1	6.4	2.1	0.936
60	4528	4	10.6	2.1	0.894
90	4447	230	12.3	2.5	0.878
120	4305	1	15.0	1.9	0.850

Advanced electro-Fenton without applied voltage (AEF_0V)					
COD					
Time (min)	mg/L	SD	% removal	SD	C/C_0 (COD)
0	5067	115			1
15	4909	112	3.0	4.4	0.969
30	4835	119	4.5	3.9	0.954
45	4760	0	6.0	2.1	0.939
60	4684	116	7.5	2.2	0.924
90	4605	230	9.1	4.0	0.909
120	4523	204	10.7	5.8	0.893

B.2 Data of variables studied affecting the efficiency of AEF process

B.2.1 Effect of reaction time

Table B.2.1.1 Raw data of residual hydrogen peroxide (H_2O_2)

Hydrogen peroxide residual		
Time (min)	mM	SD
0.0	0.00	
15.0	5.08	0.14
30.0	7.50	0.25
45.0	9.00	0.14
60.0	11.83	0.14
90.0	19.58	0.14
120.0	24.92	0.14
180.0	25.30	0.14
240.0	25.50	0.14
300.0	25.55	0.26

Table B.2.1.2 Raw data of decolorization efficiency

ADMI					
Time (min)	ADMI	SD	% removal	SD	C/C_0 (ADMI)
0	14250	250			1
15	12917	382	9.4	1.2	0.906
30	11157	382	21.7	4.2	0.783
45	8735	289	38.7	1.1	0.613
60	6243	58	56.1	0.6	0.438
90	3249	58	77.2	0.7	0.228
120	1767	58	87.6	0.5	0.124
180	1686	58	88.2	0.6	0.118
240	1543	58	89.2	0.2	0.108
300	1497	58	89.5	0.6	0.105

Table B.2.1.3 Raw data of COD reduction efficiency

COD					
Time (min)	mg/L	SD	% removal	SD	C/C_0 (COD)
0	5067	231			1
15	4319	2	14.6	4.0	0.852
30	3613	112	28.5	4.8	0.713
45	3195	233	36.9	3.9	0.631
60	2640	2	47.9	2.6	0.521
90	1647	2	67.5	2.4	0.325
120	1335	117	73.7	1.1	0.264
180	1276	114	74.8	1.9	0.252
240	1218	2	75.9	1.1	0.240
300	1161	117	77.1	1.3	0.229

B.2.2 Effect of initial pH

Table B.2.2.1 Raw data of residual hydrogen peroxide (H_2O_2)

pH2		
Hydrogen peroxide residual		
Time (min)	mM	SD
0	0.00	
15	3.88	0.13
30	4.79	0.07
45	5.92	0.07
60	8.46	0.07
90	10.08	0.14
120	11.50	0.25

pH3		
Hydrogen peroxide residual		
Time (min)	mM	SD
0	0.00	
15	5.08	0.14
30	7.50	0.25
45	9.00	0.14
60	11.83	0.14
90	19.58	0.14
120	24.92	0.14

pH4		
Hydrogen peroxide residual		
Time (min)	mM	SD
0	0.00	
15	4.17	0.07
30	5.17	0.14
45	6.67	0.07
60	9.50	0.25
90	11.96	0.07
120	13.00	0.25

pH5		
Hydrogen peroxide residual		
Time (min)	mM	SD
0	0.00	
15	3.67	0.14
30	4.21	0.07
45	5.29	0.31
60	8.13	0.22
90	9.33	0.07
120	10.17	0.58

pH7		
Hydrogen peroxide residual		
Time (min)	mM	SD
0	0.00	
15	2.04	0.07
30	3.67	0.07
45	4.71	0.07
60	5.17	0.14
90	5.83	0.14
120	6.17	0.14

pH11		
Hydrogen peroxide residual		
Time (min)	mM	SD
0	0.00	
15	0.46	0.07
30	0.87	0.01
45	0.96	0.07
60	1.29	0.07
90	1.75	0.25
120	1.92	0.07

Table B.2.2.2 Raw data of decolorization efficiency

pH2					
ADMI					
Time (min)	ADMI	SD	% removal	SD	C/C_0 (ADMI)
0	14167	144			1
15	13000	250	8.2	1.1	0.918
30	12167	144	14.1	0.1	0.859
45	11000	250	22.4	2.4	0.776
60	9500	200	32.9	0.9	0.671
90	5400	100	61.9	0.4	0.381
120	3833	58	72.9	0.7	0.271

pH3					
ADMI					
Time (min)	ADMI	SD	% removal	SD	C/C_0 (ADMI)
0	14250	250			1
15	12917	382	9.4	1.2	0.906
30	11157	382	21.7	4.2	0.783
45	8735	289	38.7	1.1	0.613
60	6243	58	56.1	0.6	0.438
90	3249	58	77.2	0.7	0.228
120	1767	58	87.6	0.5	0.124

pH4					
ADMI					
Time (min)	ADMI	SD	% removal	SD	C/C_0 (ADMI)
0	14333	144			1
15	12917	382	9.9	2.1	0.901
30	12250	500	14.5	3.6	0.855
45	11500	0	19.8	0.8	0.802
60	9467	666	33.9	4.3	0.660
90	6867	252	52.1	1.4	0.479
120	4733	115	67.0	1.1	0.330

pH5					
ADMI					
Time (min)	ADMI	SD	% removal	SD	C/C_0 (ADMI)
0	14417	144			1
15	13333	144	7.5	1.9	0.925
30	12667	144	12.1	1.6	0.879
45	12083	289	16.2	2.5	0.838
60	10333	382	28.3	3.4	0.717
90	7667	58	46.8	0.8	0.532
120	5667	58	60.7	0.7	0.393

pH7					
ADMI					
Time (min)	ADMI	SD	% removal	SD	C/C_0 (ADMI)
0	14167	144			1
15	13917	382	1.8	3.0	0.982
30	13667	144	3.5	1.7	0.965
45	12583	289	11.2	1.1	0.888
60	11667	289	17.6	2.9	0.824
90	9233	115	34.8	1.3	0.652
120	6600	100	53.4	0.4	0.466

pH11					
ADMI					
Time (min)	ADMI	SD	% removal	SD	C/C_0 (ADMI)
0	14333	289			1
15	14250	250	0.6	1.0	0.994
30	14085	500	1.7	0.0	0.994
45	14085	500	1.7	0.0	0.994
60	14085	0	1.7	0.0	0.994
90	13917	382	2.9	1.0	0.971
120	12000	250	16.3	0.9	0.837

Table B.2.2.3 Raw data of COD reduction efficiency

pH2					
COD					
Time (min)	mg/L	SD	% removal	SD	C/C_0 (COD)
0	5067	115			1
15	4671	115	7.8	2.2	0.922
30	3657	232	27.8	4.5	0.722
45	3239	117	36.1	2.2	0.639
60	2998	116	40.8	2.2	0.592
90	2506	230	50.5	4.4	0.495
120	1883	119	62.8	2.3	0.372

pH3					
COD					
Time (min)	mg/L	SD	% removal	SD	C/C_0 (COD)
0	5067	231			1
15	4319	2	14.6	4.0	0.852
30	3613	112	28.5	4.8	0.713
45	3195	233	36.9	3.9	0.631
60	2640	2	47.9	2.6	0.521
90	1647	2	67.5	2.4	0.325
120	1335	117	73.7	1.1	0.264

pH4					
COD					
Time (min)	mg/L	SD	% removal	SD	C/C_0 (COD)
0	5133	115			1
15	4667	115	9.1	0.2	0.909
30	3784	229	26.3	2.8	0.737
45	3427	115	33.3	0.7	0.668
60	2715	112	47.1	1.9	0.529
90	2342	114	54.4	1.2	0.456
120	1726	308	66.3	6.6	0.336

pH5					
COD					
Time (min)	mg/L	SD	% removal	SD	C/C_0 (COD)
0	5000	200			1
15	4521	461	9.6	8.4	0.904
30	3985	1	20.3	1.7	0.797
45	3513	115	29.7	2.0	0.703
60	2828	116	43.4	1.0	0.566
90	2489	115	50.2	3.3	0.498
120	2343	1	53.1	1.0	0.469

pH7					
COD					
Time (min)	mg/L	SD	% removal	SD	C/C_0 (COD)
0	5067	115			1
15	4860	118	4.0	3.9	0.959
30	4120	118	18.6	4.1	0.813
45	3717	230	26.7	2.8	0.734
60	3177	1	37.3	1.4	0.627
90	2708	116	46.6	2.0	0.534
120	2501	115	50.6	2.0	0.494

pH11					
COD					
Time (min)	mg/L	SD	% removal	SD	C/C_0 (COD)
0	5000	200			1
15	4983	116	0.3	2.2	0.997
30	4921	115	1.6	2.2	0.984
45	4772	1	4.6	3.9	0.954
60	4627	1	7.5	3.6	0.925
90	4435	112	11.3	2.7	0.887
120	4386	1	12.3	3.5	0.877

B.2.3 Effect of initial concentration of ferrous

Table B.2.3.1 Raw data of residual hydrogen peroxide (H_2O_2)

0.5mM		
Hydrogen peroxide residual		
Time (min)	mM	SD
0	0.00	
15	2.54	0.07
30	2.88	0.13
45	3.92	0.07
60	5.08	0.14
90	5.83	0.07
120	7.58	0.14

1mM		
Hydrogen peroxide residual		
Time (min)	mM	SD
0	0.00	
15	4.04	0.07
30	5.92	0.14
45	7.92	0.07
60	9.79	0.07
90	15.17	0.29
120	20.83	0.07

3mM		
Hydrogen peroxide residual		
Time (min)	mM	SD
0	0.00	
15	5.08	0.14
30	7.50	0.25
45	9.00	0.14
60	11.83	0.14
90	19.58	0.14
120	24.92	0.14

5mM		
Hydrogen peroxide residual		
Time (min)	mM	SD
0	0.00	
15	3.00	0.25
30	4.92	0.07
45	5.71	0.07
60	9.58	0.07
90	14.17	0.29
120	19.33	0.29

7mM		
Hydrogen peroxide residual		
Time (min)	mM	SD
0	0.00	
15	3.29	0.07
30	5.17	0.14
45	5.54	0.07
60	6.67	0.07
90	8.92	0.14
120	14.79	0.07

9mM		
Hydrogen peroxide residual		
Time (min)	mM	SD
0	0.00	
15	2.96	0.07
30	4.75	0.25
45	6.83	0.14
60	7.46	0.07
90	8.67	0.14
120	11.42	0.07

Table B.2.3.2 Raw data of decolorization efficiency

0.5mM					
ADMI					
Time (min)	ADMI	SD	% removal	SD	C/C_0 (ADMI)
0	14333	289			1
15	13917	144	2.9	2.6	0.971
30	12083	144	15.7	2.7	0.843
45	11417	289	20.3	3.7	0.797
60	11000	0	23.2	1.6	0.767
90	9867	58	31.1	1.6	0.688
120	8433	115	41.1	1.7	0.588

1mM					
ADMI					
Time (min)	ADMI	SD	% removal	SD	C/C_0 (ADMI)
0	14333	144			1
15	14083	144	1.7	1.7	0.983
30	12583	289	12.2	2.9	0.878
45	10500	250	26.7	1.2	0.733
60	8833	58	38.4	0.9	0.616
90	6767	115	52.8	1.1	0.472
120	4289	58	70.1	0.6	0.299

3mM					
ADMI					
Time (min)	ADMI	SD	% removal	SD	C/C_0 (ADMI)
0	14250	250			1
15	12917	382	9.4	1.2	0.906
30	11157	382	21.7	4.2	0.783
45	8735	289	38.7	1.1	0.613
60	6243	58	56.1	0.6	0.438
90	3249	58	77.2	0.7	0.228
120	1767	58	87.6	0.5	0.124

5mM					
ADMI					
Time (min)	ADMI	SD	% removal	SD	C/C_0 (ADMI)
0	14231	144			1
15	13826	289	2.8	2.7	0.972
30	13036	500	8.4	2.7	0.916
45	12106	144	14.9	1.0	0.851
60	10015	500	29.6	2.9	0.704
90	7690	100	46.0	0.9	0.540
120	4900	200	65.4	1.7	0.344

7mM					
ADMI					
Time (min)	ADMI	SD	% removal	SD	C/C_0 (ADMI)
0	14251	144			1
15	13966	289	2.0	2.6	0.980
30	13680	289	4.0	2.6	0.960
45	12826	144	10.0	1.6	0.900
60	11400	144	20.3	0.9	0.800
90	9690	100	32.0	1.3	0.680
120	6900	100	51.2	0.9	0.484

9mM					
ADMI					
Time (min)	ADMI	SD	% removal	SD	C/C_0 (ADMI)
0	14253	144			1
15	14180	144	0.5	1.7	0.995
30	13826	144	3	1.0	0.970
45	12545	144	11.9	1.6	0.880
60	10830	289	24.3	1.7	0.760
90	9196	58	36.4	0.9	0.645
120	7270	58	48.2	0.8	0.510

Table B.2.3.3 Raw data of COD reduction efficiency

0.5mM					
COD					
Time (min)	mg/L	SD	% removal	SD	C/C_0 (COD)
0	5027	162			1
15	4959	200	1.34	1.1	0.987
30	4221	117	16.0	1.0	0.840
45	3937	1	21.6	2.5	0.783
60	3852	114	23.3	3.1	0.766
90	3573	115	28.9	3.4	0.711
120	3212	114	36.0	4.2	0.639

1mM					
COD					
Time (min)	mg/L	SD	% removal	SD	C/C_0 (COD)
0	5133	115			1
15	4784	119	6.8	1.8	0.932
30	3787	232	26.2	4.1	0.738
45	2993	115	41.7	3.2	0.583
60	2780	115	45.8	1.2	0.542
90	2178	230	57.6	4.1	0.424
120	1946	229	62.1	4.1	0.379

3mM					
COD					
Time (min)	mg/L	SD	% removal	SD	C/C_0 (COD)
0	5067	231			1
15	4319	2	14.6	4.0	0.852
30	3613	112	28.5	4.8	0.713
45	3195	233	36.9	3.9	0.631
60	2640	2	47.9	2.6	0.521
90	1647	2	67.5	2.4	0.325
120	1335	117	73.7	1.1	0.264

5mM					
COD					
Time (min)	mg/L	SD	% removal	SD	C/C_0 (COD)
0	5133	115			1
15	4469	232	12.8	6.6	0.871
30	4172	114	18.7	2.0	0.813
45	3807	117	25.8	3.4	0.742
60	3310	230	35.5	5.4	0.645
90	2663	119	48.1	2.0	0.519
120	2134	115	58.4	1.9	0.416

7mM					
COD					
Time (min)	mg/L	SD	% removal	SD	C/C_0 (COD)
0	5067	115			1
15	4681	115	7.6	2.2	0.924
30	4051	113	20.0	2.1	0.799
45	3911	1	22.8	1.8	0.772
60	3293	1	35.0	1.5	0.650
90	2658	398	47.4	8.8	0.525
120	2497	115	50.7	3.3	0.493

9mM					
COD					
Time (min)	mg/L	SD	% removal	SD	C/C_0 (COD)
0	5000	200			1
15	4486	230	10.1	8.0	0.897
30	4057	116	18.8	4.0	0.811
45	3957	117	20.7	5.4	0.791
60	3881	1	22.3	3.1	0.776
90	3328	232	33.3	7.0	0.666
120	2618	1	47.6	2.1	0.524

B.2.4 Effect of applied voltage

Table B.2.4.1 Raw data of residual hydrogen peroxide (H_2O_2)

1.0V		
Hydrogen peroxide residual		
Time (min)	mM	SD
0	0.00	
15	4.58	0.07
30	8.75	0.25
45	10.58	0.07
60	12.75	0.25
90	17.33	0.07
120	21.67	0.14

2.0V		
Hydrogen peroxide residual		
Time (min)	mM	SD
0	0.00	
15	5.08	0.14
30	7.50	0.25
45	9.00	0.14
60	11.83	0.14
90	19.58	0.14
120	24.92	0.14

3.0V		
Hydrogen peroxide residual		
Time (min)	mM	SD
0	0.00	
15	3.96	0.07
30	4.25	0.25
45	7.00	0.25
60	9.42	0.14
90	12.42	0.07
120	17.50	0.25

4.0V		
Hydrogen peroxide residual		
Time (min)	mM	SD
0	0.00	
15	0.54	0.19
30	0.75	0.25
45	0.96	0.07
60	1.50	0.25
90	2.54	0.07
120	3.79	0.07

Table B.2.4.2 Raw data of decolorization efficiency

1.0V					
ADMI					
Time (min)	ADMI	SD	% removal	SD	C/C_0 (ADMI)
0	14246	144			1
15	13615	250	4.7	2.0	0.956
30	11855	289	15.9	1.8	0.832
45	10045	250	29.4	1.2	0.705
60	8536	58	39.8	0.5	0.599
90	6965	58	51.1	0.9	0.489
120	5100	100	64.0	0.8	0.358

2.0V					
ADMI					
Time (min)	ADMI	SD	% removal	SD	C/C_0 (ADMI)
0	14250	250			1
15	12917	382	9.4	1.2	0.906
30	11157	382	21.7	4.2	0.783
45	8735	289	38.7	1.1	0.613
60	6243	58	56.1	0.6	0.438
90	3249	58	77.2	0.7	0.228
120	1767	58	87.6	0.5	0.124

3.0V					
ADMI					
Time (min)	ADMI	SD	% removal	SD	C/C_0 (ADMI)
0	14333	144			1
15	13583	144	5.2	0.1	0.948
30	12917	289	9.9	1.1	0.901
45	12083	144	15.7	1.6	0.843
60	11000	250	23.3	1.1	0.767
90	8733	58	39.1	0.2	0.609
120	6300	100	56.0	0.4	0.440

4.0V					
ADMI					
Time (min)	ADMI	SD	% removal	SD	C/C_0 (ADMI)
0	14417	144			1
15	13600	144	5.7	2.0	0.943
30	12950	144	10.2	0.9	0.898
45	12000	144	16.8	0.2	0.832
60	11760	144	18.4	0.9	0.816
90	10000	289	30.6	1.3	0.694
120	9033	58	37.3	0.6	0.627

Table B.2.4.3 Raw data of COD reduction efficiency

1.0V					
COD					
Time (min)	mg/L	SD	% removal	SD	C/C_0 (COD)
0	5000	200			1
15	4727	1	5.4	3.8	0.945
30	4260	4	14.7	3.5	0.852
45	3964	116	20.6	4.0	0.793
60	3663	227	26.8	2.5	0.733
90	3190	230	36.0	6.8	0.638
120	2654	2	46.9	2.1	0.531

2.0V					
COD					
Time (min)	mg/L	SD	% removal	SD	C/C_0 (COD)
0	5067	231			1
15	4319	2	14.6	4.0	0.852
30	3613	112	28.5	4.8	0.713
45	3195	233	36.9	3.9	0.631
60	2640	2	47.9	2.6	0.521
90	1647	2	67.5	2.4	0.325
120	1335	117	73.7	1.1	0.264

3.0V					
COD					
Time (min)	mg/L	SD	% removal	SD	C/C_0 (COD)
0	5200	346			1
15	4936	1	5.1	5.9	0.949
30	4532	4	12.6	5.5	0.872
45	4488	4	13.4	5.5	0.863
60	4176	230	19.4	8.5	0.803
90	3935	115	24.0	7.0	0.757
120	3587	231	30.9	4.7	0.690

4.0V					
COD					
Time (min)	mg/L	SD	% removal	SD	C/C_0 (COD)
0	5067	231			1
15	4791	3	5.3	4.5	0.946
30	4521	227	10.7	4.3	0.892
45	4484	1	11.5	4.0	0.885
60	4302	4	15.1	3.9	0.849
90	4093	117	19.2	1.4	0.808
120	3896	230	23.1	6.7	0.769

BIOGRAPHY

Name	Ms. Preenaphan Tanteerapolchai
Date of Birth	May 7, 1996
Education	2017: Bachelor of Engineering, (Environmental Engineering), King's Mongkut University of Technology Thonburi 2020: Master of Engineering, (Engineering Technology), Sirindhorn International Institute of Technology, Thammasat University

Publication

Tanteerapolchai, P., Sreearunothai, P., Sombatmankhong, K. Saisriyoot, M. (2020). Decolorization and COD Reduction of Effluent from Biogas Chamber. Proceeding of 9^{th} *International Conference on Environmental Engineering, Science and Management,* 1-8.